nature chemical biology

Allosteric communication between protomers of dopamine class A GPCR dimers modulates activation

Yang Han[1–3], Irina S Moreira[4], Eneko Urizar[1–3], Harel Weinstein[4,5] & Jonathan A Javitch[1–3,6]

A major obstacle to understanding the functional importance of dimerization between class A G protein–coupled receptors (GPCRs) has been the methodological limitation in achieving control of the identity of the components comprising the signaling unit. We have developed a functional complementation assay that enables such control, and we demonstrate it here for the human dopamine D2 receptor. The minimal signaling unit, two receptors and a single G protein, is maximally activated by agonist binding to a single protomer, which suggests an asymmetrical activated dimer. Inverse agonist binding to the second protomer enhances signaling, whereas agonist binding to the second protomer blunts signaling. Ligand-independent constitutive activation of the second protomer also inhibits signaling. Thus, GPCR dimer function can be modulated by the activity state of the second protomer, which for a heterodimer may be altered in pathological states. Our new methodology also makes possible the characterization of signaling from a defined heterodimer unit.

A number of open questions about the functional mechanisms of GPCRs center on the role of dimerization, its physiological significance and its pharmacological consequences[1]. Many of the pertinent results from the literature describe (i) effects that have been attributed to activating one receptor in the presence of another[2] and (ii) the ability to modulate activity of one receptor using ligands targeting the second receptor[3,4]. Compelling as these examples are, it has thus far been difficult to construct a mechanism that would coherently explain all these phenomena. For most GPCRs, a major obstacle has been methodological, especially the inability to control the identity of the components of the G protein signaling unit, which must include the interacting receptors and G proteins. Here we present a mechanism for rhodopsin-like class A GPCRs that we were able to identify using a new approach that enabled us to control the identity of the participants in the signaling complex.

In class C GPCRs, such control has been possible because of the unique cell biology of the $GABA_B$ receptor. The R2 subunit does not signal by itself in response to γ-aminobutyric acid (GABA, **1**) but is essential for surface expression of the R1 subunit and therefore for signaling of the heterodimeric complex[5]. Therefore, the only species on the surface that can signal must contain R1 and R2, which allows the study of defined heterodimers. These receptors have been shown to function through a "transactivation" mechanism in which a GABA-binding R1 signals through interactions of R2 with G protein[5]. A clever adaptation of the endoplasmic reticulum retention signal from the $GABA_B$ receptor has enabled controlled cell surface expression and study of signaling by defined metabotropic glutamate receptor (mGluR) "hetero"-dimers[6], which have been inferred to signal through *trans* activation and through *cis* activation, in which the agonist-bound receptor interacts directly with G protein[6]. Such an approach to engineered endoplasmic reticulum retention signals has not yet been successful in class A receptors, but class A glycoprotein hormone receptors with large extracellular binding domains also appear to be capable of both *trans* and *cis* activation[7].

So far, the native functional signaling unit in other class A rhodopsin-like receptors remains unclear. Indeed, both rhodopsin[8] and the β_2-adrenergic receptor (B2AR)[9] have been shown to signal efficiently to G proteins when reconstituted into lipid nanodiscs containing only a single receptor. Thus, after solubilization and reconstitution, these GPCRs can function alone. Nevertheless, such studies cannot determine whether these receptors do function alone *in vivo*, and this question must be addressed directly through an exploration of signaling in their native organization. A number of studies have shown that coexpression of two different class A GPCRs can lead to signaling properties that differ from their properties when expressed alone[10,11]. However, it is not possible from such studies to differentiate downstream integration of signaling from an actual heteromeric signaling unit in which the two protomers interact directly to modulate signaling.

Evidence for association of conformational change at a homodimer interface with activation state[12] supports state-dependent communication between protomers and a potential role for interprotomer modulation of signaling. However, in contrast to findings for the class C $GABA_B$ and mGlu receptors and the class A receptors with large N-terminal binding sites (thyrotropin (TSH), follicle-stimulating hormone (FSH) and luteinizing hormone (LH) receptors), results for the rhodopsin-like leukotriene B_4 receptor BLT1 support the existence of *cis* but not *trans* activation, with no functional role identified for

[1]Center for Molecular Recognition and [2]Department of Psychiatry, Columbia University College of Physicians and Surgeons, New York, New York, USA. [3]Division of Molecular Therapeutics, New York State Psychiatric Institute, New York, New York, USA. [4]Department of Physiology and Biophysics and [5]The HRH Prince Alwaleed Bin Talal Bin Abdulaziz Alsaud Institute for Computational Biomedicine, Weill Cornell Medical College, Cornell University, New York, New York, USA. [6]Department of Pharmacology, Columbia University College of Physicians and Surgeons, New York, New York, USA. Correspondence should be addressed to J.A.J. (jaj2@columbia.edu).

Received 22 October 2008; accepted 28 April 2009; published online 2 August 2009; doi:10.1038/nchembio.199

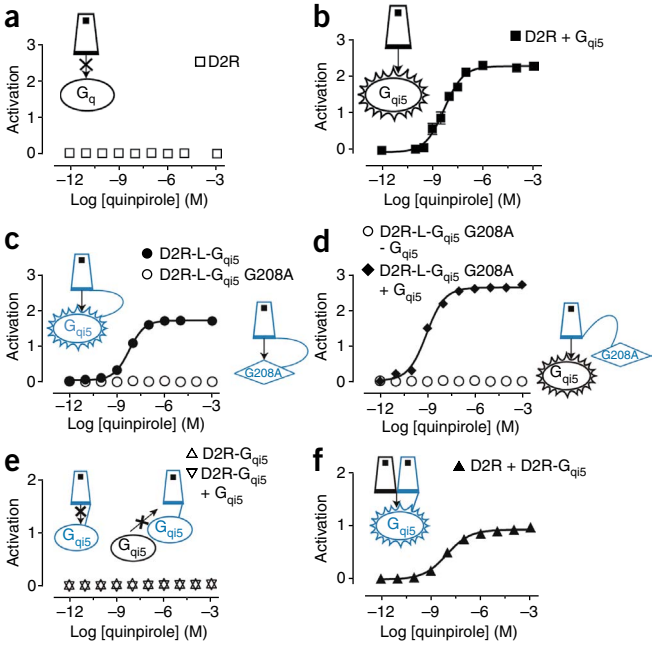

Figure 1 Functional complementation of two 'nonfunctional receptors'. We used an aequorin assay that couples G_q (or G_{qi5}) activation to a luminescence readout. (**a**) The agonist quinpirole did not lead to D2R-induced G_q activation. (**b**,**c**) D2R when coexpressed with free G_{qi5} (**b**) or D2R fused with G_{qi5} via a linker (D2-linker-G_{qi5}) (**c**) led to quinpirole-induced luminescence. (**c**) A guanine nucleotide exchange–deficient Gα fusion construct, D2-linker-G_{qi5} G208A, failed to produce luminescence. (**d**) Free G_{qi5} rescued the function of D2-linker-G_{qi5} G208A. (**e**) Free G_{qi5} failed to rescue the function of nonlinker D2R-G_{qi5}, which unlike D2R-linker-G_{qi5} did not signal when expressed alone. (**f**) Coexpressing D2R with D2R-G_{qi5} (12 h tetracycline induction) restored signaling, despite the inability of either construct to signal in this assay when expressed alone. Activation data represent luminescence relative to that seen with 0.1% (v/v) triton treatment. The means ± s.e.m. of at least three experiments, each conducted in triplicate, are shown. The symbols used in **Figures 1**–**4** and **6** are explained in detail in **Supplementary Figure 2**.

the second protomer, despite evidence that it changes conformation in response to agonist binding to its dimer partner[13,14].

Receptor–G protein fusion constructs, in which the C terminus of a GPCR is fused to the N terminus of Gα, have been used to explore receptor signaling[15–18]. Coexpression of such GPCR–G protein fusions with a second GPCR has been used to study heterodimer signaling; in such a scenario the unfused GPCR can activate the G protein fused to a coexpressed GPCR[15–17]. However, the participants in the signaling unit are not identifiable in this experimental protocol because coexpression of GPCRs leads to a combination of different signaling units consisting of both homodimers and heterodimers. Indeed, a tethered G protein fused to a single membrane-spanning segment can be activated efficiently by a coexpressed GPCR[16,19], which suggests that a GPCR–G protein fusion construct might provide G protein for activation by another receptor, or another dimer of receptors, without directly participating in the relevant dimeric signaling unit. The long cytoplasmic tails and flexible linkers through which G proteins have been fused to GPCRs are likely to allow promiscuous interactions that exacerbate this problem. Indeed, the tether attaching the B2AR to fused G_s can be substantially shortened with preserved function[20], but it remains unknown whether the G protein in this case is activated by the receptor to which it is covalently attached or by another receptor.

Here we have developed a functional complementation assay that allows us to control the components of the human dopamine D2 receptor (D2R) signaling unit and thus to explore the dimeric functional unit and the individual contributions from each GPCR protomer to G protein signaling. Our system reports directly on receptor–G protein interactions, which allows us to rule out downstream crosstalk as the mechanism of modulation of G protein function upon coexpression of different partner receptors. This new methodology allowed us to propose a mechanistic explanation for the reciprocal modulation of protomer functions in a dimeric signaling complex. The minimal signaling unit, which consists of two GPCRs and a single heterotrimeric G protein, appears to be maximally activated by agonist binding to a single protomer, which suggests an asymmetrical activated dimer. Indeed, agonist binding to the second protomer blunts signaling, whereas inverse agonist binding to the second protomer enhances signaling. Such allosteric modulation of one protomer by the state of the other also has important ramifications for pharmacological manipulation of GPCR heterodimers. The observation that a nonbinding constitutively active receptor blunts signaling of a coexpressed wild-type (WT) receptor highlights the importance of the conformational state of the second protomer. Therefore, GPCR heterodimer function is modulated not only by ligand binding to the second protomer but also by its ligand-independent constitutive activity; both types of modulation may be altered in pathological states.

RESULTS

Engineering a luminescence readout for D2R activation

To isolate signaling of the D2R (a prototypical G_o- or G_i-coupled receptor) from endogenous G proteins and to control each of the components of the signaling complex, we engineered Flp-In T-REx 293 cells to stably express aequorin (AEQ cells) (see Methods). Aequorin produces luminescence in a calcium-dependent manner in the presence of the substrate coelenterazine[21] (**2**), and it has been used to create a sensitive luminescence readout for GPCR-mediated phospholipase C activation[22]. In these cells, endogenous muscarinic or purinergic receptors signaled robustly via endogenous G_q, resulting in strong agonist-induced (acetylcholine (ACH, **3**) and ATP (**4**), respectively) luminescence signals (**Supplementary Fig. 1a**). In contrast, when D2R was stably expressed in AEQ cells, treatment with the agonist quinpirole (**5**) did not lead to luminescence, which is consistent with a lack of D2R coupling to G_q (**Fig. 1a** and **Supplementary Fig. 2**).

To couple D2R activation to a luminescence readout in these cells, we expressed a chimeric, pertussis toxin (PTX)-resistant G_q (G_{qi5}) that could signal from G_i-coupled receptors[23] (see Methods). D2R signaled robustly when stably coexpressed with free G_{qi5} or when fused at its C terminus to G_{qi5} through an eight-amino-acid linker (D2-linker-G_{qi5}) (**Fig. 1b**,**c**). The increase in luminescence was unaffected by PTX (**Supplementary Fig. 1b**), whereas a mutation in G_{qi5} (G_{qi5} G208A) that prevents GTP-induced Gα activation[24] prevented the luminescence response to D2R activation (**Fig. 1c**). No quinpirole response was seen when free G_{qi5} was expressed without D2R (data not shown), which is consistent both with the absence of endogenous D2R in these cells and with the lack of other targets for quinpirole-mediated signaling.

Curiously, expression of free G_{qi5} fully rescued the function of D2-linker-G_{qi5} G208A (**Fig. 1d**), which indicates that the linker afforded sufficient flexibility for the nonfunctional G protein to swing away and permit a free functional G_{qi5} to interact and to restore agonist-mediated signaling. Therefore, we could not use the D2-linker-G_{qi5} construct to monitor functional coupling of two

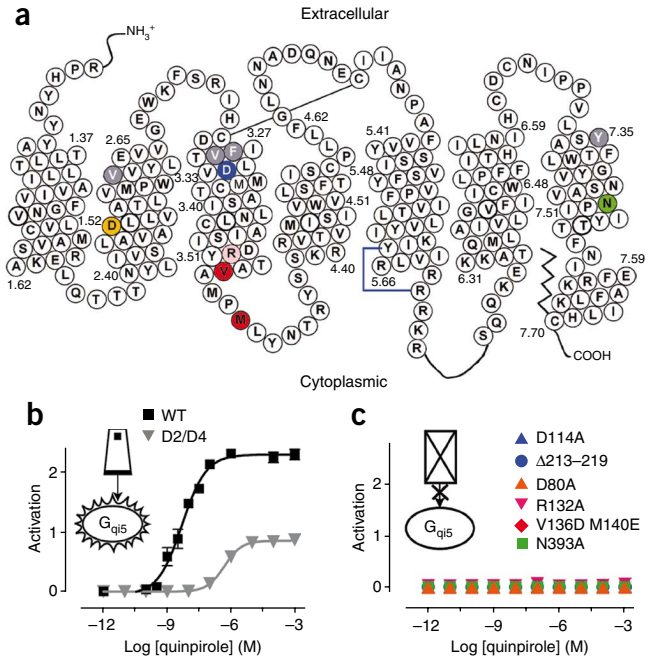

Figure 2 Characterization of D2R mutants. (**a**) Schematic representation showing the positions of the mutations in the D2 receptor. (**b**) D2/D4, a D2 mutant with four amino acids substituted from the D4 receptor ($V91^{2.61}F$, $F110^{3.29}L$, $V111^{3.28}M$ and $Y408^{7.35}V$), making it 1,000 times more sensitive to a D4-selective inhibitor (**Supplementary Fig. 4**), is activated by quinpirole, albeit with a lower potency and efficacy when compared with WT D2R. (**c**) All the other mutants, which are described in the text, were nonfunctional. Activation data were normalized as in **Figure 1**. Coloring in **a** corresponds to the symbols and lines in **b** and **c**. The means ± s.e.m. of at least three experiments, each conducted in triplicate, are shown.

defined protomers, since the flexibility of the linker might allow this construct to provide the Gα to another protomer (or to another dimer of protomers) without the actual participation of the fused receptor in the signaling unit.

To address this problem, we developed another D2R-G_{qi5} construct in which the linker was removed and G_{qi5} was fused more directly to the short cytoplasmic tail of the D2R (D2-G_{qi5}). This construct expressed at the plasma membrane (**Supplementary Fig. 3a**,**b**), but agonist treatment failed to produce luminescence (**Fig. 1e**). We hypothesized that the lack of signaling resulted from the inability of the short-tethered Gα to be positioned appropriately for a productive interaction either with the cytoplasmic loops of the receptor to which it was fused, or with a second protomer. Indeed, in contrast to the D2-linker-G_{qi5}, D2-G_{qi5} signaling was not rescued by free G_{qi5} (**Fig. 1e**), most likely because the tethered Gα sterically blocks free G_{qi5} from making a productive interaction with the cytoplasmic loops of the fused receptor.

Notably, however, coexpression in the AEQ cells of D2R (termed 'protomer A') and D2-G_{qi5} ('protomer B'), each of which is incapable of signaling in our assay when expressed alone, led to robust agonist-mediated receptor activation (**Fig. 1f**), which indicates that when activated, the fused G_{qi5} is fully capable of interacting with phospholipase C. That this effect was mediated solely by the fused G_{qi5} and not by endogenous G_i or G_o was demonstrated by the lack of effect of PTX treatment on activation (**Supplementary Fig. 1c**). This reconstitution of a signaling unit from two 'nonfunctioning' class A GPCR protomers provided us with the unique opportunity to manipulate each protomer independently and to determine its role in signaling while eliminating the contribution of homodimers. These experiments do not rule out a higher order receptor complex, but in the simplest scenario, the minimal signaling unit is composed of protomer A, protomer B and the G protein fused to protomer B (**Fig. 1f**), and for simplicity, we will subsequently refer to this receptor complex as a 'dimer'. The extremely close proximity between these protomers and the inability of protomer B to signal to its own fused G protein or to a neighboring fused G protein indicates that only one G protein serves this signaling unit of two GPCRs. Our inferences regarding the signaling unit are entirely consistent with the results from our parallel computational modeling studies (see below). These modeling studies make the essential point that the relatively large size of the G protein heterotrimer matches the cytoplasmic surfaces of at least two neighboring GPCR protomers.

Revealing asymmetry of signaling

In order to experimentally manipulate the function of each protomer in the dimeric unit, we constructed a panel of D2R mutants predicted to be binding- and activation-deficient based on findings in the literature for related class A GPCRs. These include $D114^{3.32}A$, which does not bind agonists or antagonists[25]; $R132^{3.50}A$ (ref. 26) and $V136^{3.54}D$ $M140^{3.58}E$ in intracellular loop (IL) 2 (ref. 27); deletion of amino acids 213–219 in IL3 (ref. 28); and $D80^{2.50}A$ (previously characterized in D2R)[29] and $N393^{7.49}A$ (ref. 30) in the membrane-spanning segments (**Fig. 2a**), all of which were expected to disrupt agonist-mediated G protein activation. We also expressed the D2R mutant $V91^{2.61}F$ $F110^{3.29}L$ $V111^{3.28}M$ $Y408^{7.35}V$ (termed D2/D4) (**Fig. 2a**), which, unlike WT D2R, is potently inhibited by the selective D4 antagonist L745,870 (ref. 31) (**6**) (**Supplementary Fig. 4**). Each of these constructs expressed at the plasma membrane (**Supplementary Fig. 3**). In contrast to the robust activation of WT, we observed a reduction in potency and a large decrease in maximal activation by quinpirole in D2/D4 when expressed with free G_{qi5} (**Fig. 2b**). As anticipated, none of the mutants deficient in binding or signaling led to agonist-mediated luminescence when placed into an unfused D2R construct coexpressed with free G_{qi5} (**Fig. 2c**), or when the mutations were placed in the D2-linker-G_{qi5} construct and expressed alone (**Supplementary Fig. 5**).

When D2/D4 was expressed as protomer A with WT D2R-G_{qi5} as protomer B, we observed a reduction in potency and a large decrease in maximal activation by quinpirole (**Fig. 3a**), which is similar to its signaling properties when expressed with free G_{qi5} (**Fig. 2b**) (these and all subsequent activation data were normalized for surface expression of protomer B; see Methods and **Supplementary Figs. 3** and **6**). Expression of any of the nonbinding or nonsignaling receptor mutants as protomer A completely prevented activation (**Fig. 3b**), despite the presence of WT D2R-G_{qi5} in protomer B. Thus, protomer A, which must interact with the Gα provided by protomer B, appears to play a dominant role in the activation process. Note that the absence of *trans* activation was not a result of our functional complementation system or lack of sufficient mobility of fused G protein; we also failed to see evidence for *trans* activation even when nonbinding and noncoupling receptors (without G protein fusions) were co-expressed with free G_{qi5} (data not shown).

In contrast, we observed robust agonist-mediated activation with WT D2R as protomer A and D2/D4-G_{qi5} (**Fig. 3c**) or D114A-G_{qi5} (**Fig. 3d**) as protomer B. These data suggest that agonist binding to protomer A is sufficient for normal activation (see below), and they imply an asymmetric organization of the signaling complex

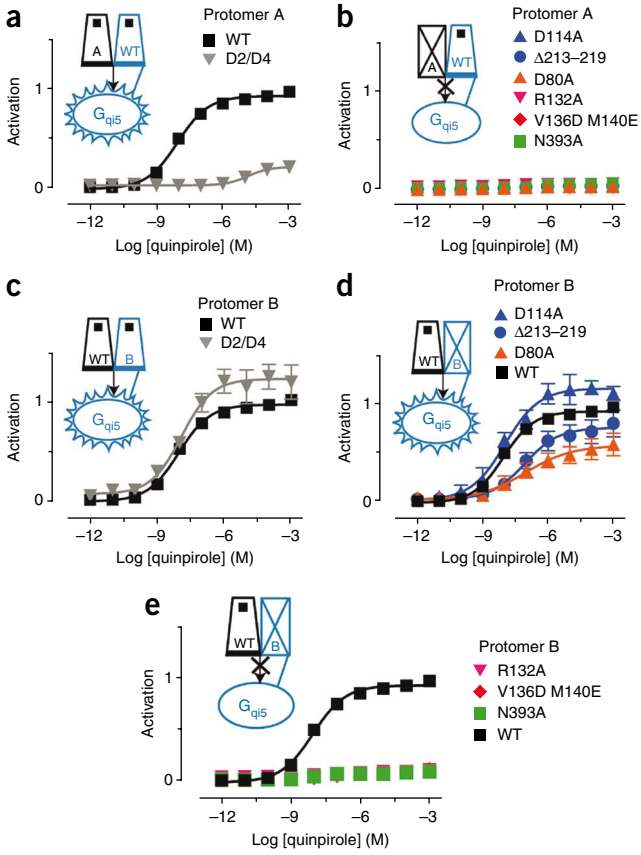

Figure 3 Asymmetric contributions of the protomers to signaling. (**a**) When all mutants (as protomer A) were coexpressed with WT D2R-G_{qi5} (as protomer B), only WT and D2/D4 were able to signal. (**b**) None of the other mutants were able to restore signaling when coexpressed with WT D2R-G_{qi5}. (**c**–**e**) The results differed when WT D2R (as protomer A) was coexpressed with the various mutant-G_{qi5} constructs (as protomer B). (**c**) D2/D4-G_{qi5} (gray inverted triangle) restored the ability of unfused WT D2R to signal. (**d**) D114$^{3.32}$A-G_{qi5} (blue triangle), deletion 213–219-G_{qi5} (blue circle) and D80$^{2.50}$A-G_{qi5} (orange triangle) also restored the ability of unfused WT D2R to signal. (**e**) Coexpressing R132$^{3.50}$A-G_{qi5} (magenta inverted triangle), V136$^{3.54}$D M140$^{3.58}$E-G_{qi5} (red diamond) or N393$^{7.49}$A-G_{qi5} (green square) with WT D2R failed to rescue signaling. Note that D114A-G_{qi5} (blue triangle) and D2/D4-G_{qi5} (gray inverted triangle) showed a higher maximal activation than WT. Activation data represent relative luminescence when compared to WT D2R coexpressed with WT D2R-G_{qi5} after normalizing for surface expression of the G_{qi5} fusion construct (see Methods). The means ± s.e.m. of at least three experiments, each conducted in triplicate, are shown.

comprising two GPCR protomers with G protein. When R132$^{3.50}$A-G_{qi5} or V136$^{3.54}$D M140$^{3.58}$E-G_{qi5} was expressed as protomer B with WT D2R as protomer A, no activation was observed (**Fig. 3e**). In contrast, although the IL3 deletion construct abolished activation when placed in protomer A (**Fig. 3b**), it supported signaling when coexpressed as protomer B (fused to G_{qi5}) along with WT D2 as protomer A (**Fig. 3d**). These data support a mechanism in which two GPCRs activate a single G protein through interactions that involve IL2 from both protomers, whereas IL3 from only one protomer is essential for signaling. Note that the failure of R132$^{3.50}$A-G_{qi5} or V136$^{3.54}$D M140$^{3.58}$E-G_{qi5} to function with WT is not due to an inability of these protomers to interact, since we observed efficient bioluminescence resonance energy transfer as well as bimolecular luminescence and fluorescence complementation[32] between these mutants and WT D2R (**Supplementary Fig. 7**).

To explore the nature of the conformational changes in the dimeric receptor unit, we also studied inactivating mutations within the membrane-spanning segments. The transduction-uncoupling mutants D80$^{2.50}$A and N393$^{7.49}$A revealed additional differences in the roles of protomers A and B. When either of these mutations was placed in protomer A, signaling was abolished, which is consistent with the dominant role of this protomer (**Fig. 3b**). In contrast, when placed in protomer B, D80$^{2.50}$A-G_{qi5} signaled when coexpressed with WT D2R as protomer A (**Fig. 3d**), whereas N393$^{7.49}$A-G_{qi5} did not (**Fig. 3e**). These results suggest that the nature of the conformational changes in protomer B during activation differs from that in protomer A.

The activation state of protomer B modulates signaling

Agonist binding to only protomer A and not protomer B produced full activation, as coexpressed D2R and D114$^{3.32}$A-G_{qi5} were robustly activated by quinpirole (**Fig. 3d**). Moreover, it appeared that binding of a second agonist to protomer B might inhibit signaling, as coexpression of both WT D2R and D2R-G_{qi5} led to lower maximal activation than did D2R coexpressed with D114$^{3.32}$A-G_{qi5} (**Fig. 3d**). We tested this hypothesis using the D2/D4 chimeric receptor. As predicted, when D2/D4 was expressed as protomer A with D2R-G_{qi5} as protomer B, quinpirole's ability to bind and activate was blocked by the D4-selective antagonist L745,870, reflecting the primacy of protomer A (**Fig. 4a**). In contrast, coexpressing D2/D4-G_{qi5} as protomer B with D2R as protomer A led to robust receptor activation that was greater than that seen with WT D2R and D2R-G_{qi5} (**Fig. 3c**), and that was further enhanced in the presence of L745,870 (**Fig. 4b**), which blocks quinpirole binding to protomer B but not protomer A.

It is the active conformation of the second protomer that inhibits signaling and not agonist binding *per se*. This is evidenced by the finding that activating protomer B by constitutively activating mutations (**Supplementary Fig. 8**) in a nonbinding receptor (D114$^{3.32}$A E339$^{6.30}$A T343$^{6.34}$R-G_{qi5})[26,33] substantially reduced the signaling efficacy of a WT protomer A (**Fig. 4c**). Thus, activation of the second protomer, either by ligand binding or by its inherent constitutive activity, inhibits signaling by its partner.

Computational modeling of the D2R–G protein interface

Because our experimental findings require a structural context in which the new mechanisms for GPCR–G protein interactions emerging from this study can be understood, we carried out independent computational studies that combined molecular modeling with experimental data available in the literature about the modes of interaction of the component GPCRs and G protein but without direct reference to the new findings. We used information available from the current crystal structures of GPCRs and specific data about inactive and activated states for bovine rhodopsin because, unlike the D2R, such a structural template is accompanied by much experimental data about details of the sites and mode of interaction with G proteins to guide protein-protein docking. Thus, we took advantage of experimental data from cross-linking, alanine scanning mutagenesis, and other structural and functional studies of the GPCR–G protein interfaces pointing to several amino acid residues likely to be involved in complex formation between rhodopsin and the G protein α and βγ subunits (**Supplementary Methods**). The data derived from the literature were used not only as constraints to guide docking of transducin (G_t) to a variety of dimer models of rhodopsin (**Supplementary Fig. 9**) but also to screen for the oligomerization solution that best satisfied these constraints, as detailed in the Methods.

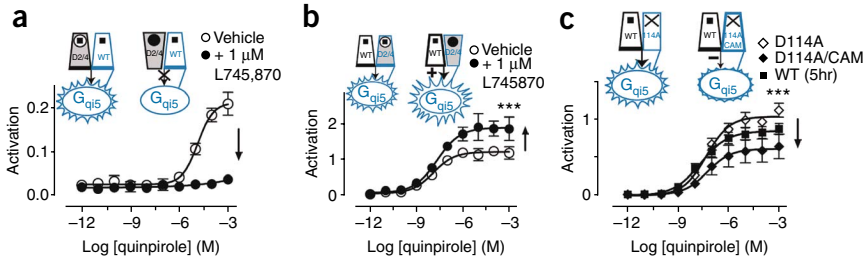

Figure 4 The second protomer allosterically modulates signaling. (**a**,**b**) Shown are effects on signaling with the D2/D4 construct expressed either as protomer A (**a**) or as protomer B (D2/D4-G_{qi5}) (**b**). (**a**) The D4-selective antagonist L745,870 (1 μM) totally blocked signaling of the D2/D4 construct expressed as protomer A with WT-G_{qi5}. (**b**) In contrast, L745,870 increased maximal activation for WT D2R coexpressed with D2/D4-G_{qi5} to 156.7 ± 7.3% ($n = 9$) ($P < 0.01$*** by Student's *t*-test) of that observed for D2R coexpressed with WT D2R-G_{qi5} (**Fig. 3a**). (**c**) Coexpression of a constitutively active mutant (**Supplementary Fig. 8**) that was unable to bind ligand ($D114^{3.32}A$/CAM-G_{qi5}), to enhance the fraction of protomer B in an active conformation, led to 49.6 ± 8.4% ($n = 9$) ($P < 0.01$*** by Student's *t*-test) of maximal activity (filled diamonds) when compared to WT D2R coexpressed with D114A-G_{qi5} (open diamonds). Activation data were normalized to surface expression as described in **Figure 3**. The means ± s.e.m. of at least three experiments, each conducted in triplicate, are shown.

Both TM4/TM5 and TM1 have been implicated in D2R oligomerization[12,32,34]. In order to discriminate between a functional dimer with an interface involving TM4 and TM5 (named TM4,5 dimer) from one with a TM1 interface (TM1 dimer), we docked the molecular structure of transducin to a rhodopsin nonamer (**Fig. 5a**; **Supplementary Fig. 9**) subject to specific constraints for the interaction between G_t and the central rhodopsin (**Supplementary Table 1**). As described in the Methods, transducin was free to rotate in any direction around this central rhodopsin to select any one of the dimeric forms in the array. The G_t could select a second protomer from the oligomeric structure in which the GPCR interface corresponds to either a TM4,5 interface or a TM1 interface dimer. The probability for G_t selecting either dimer interface was compared in a scan for optimal interaction carried out on the oligomeric structure shown in **Figure 5a** and **Supplementary Figure 9**. The complexes resulting from this scan were considered acceptable (and counted) only if the underlying structural models satisfied at least 50% of the experimentally based constraints (set 1 in **Supplementary Table 2**). A substantial fraction of TM4, 5 dimers (21.1%) satisfied this cutoff, but no complex with a TM1 dimer met the filtering criteria.

A possible mode of oligomer reorganization associated with function had been suggested based on crosslinking studies in D2R[34] and rhodopsin[35]. To evaluate the functional impact of such a reorganization, G_t was docked to the TM4,5 and TM4 dimer alternatives (**Supplementary Fig. 9**). The Cα-Cα distances for specific interactions between rhodopsin and transducin in the optimal representative structures of the 1,000 structures obtained for each alternative in this dimer docking procedure (see Methods for details) are summarized in **Supplementary Table 2**. For these optimal structures, the sets of Cα-Cα distances are very similar, but the frequency of appearance of optimally positioned complexes is much higher for model 2 (TM4 dimer; 76.1%) than for model 1 (TM4,5 dimer; 23.8%). This is evident from the average values of the distances (**Supplementary Table 1**), which are mostly larger in model 1 than in model 2 constructs. Thus, model 2 is considered the better representation of the GPCR dimer complex with the G protein in the context of the oligomeric arrangement. This is consistent with the proposed transition from a TM4,5 interface to a TM4 interface upon activation (which is suggested by crosslinking results for the D2R[34]) and indicates the relation between optimal G protein binding to the dimer and an activated state.

Notably, in the optimal G protein–dimer complex, the cytoplasmic ends of TM3 and IL2 from both protomers interact with the docked G protein. This is shown in **Figure 5** for model 2 but holds as well for model 1. In contrast, only IL3 from protomer A, but not from protomer B, contacts the docked Gα, which is consistent with our experimental results showing that an inactivating IL3 mutation is tolerated in protomer B but not in protomer A.

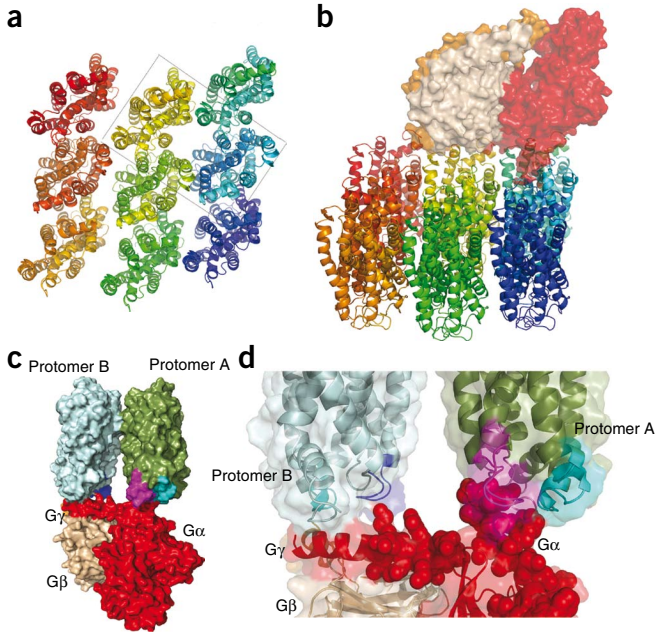

Figure 5 Computational model of the complex between the rhodopsin dimer and heterotrimeric G_t. (**a**) Structural representation of the nonameric oligomer array; the dashed box identifies the TM4 dimer contained in model 2. (**b**) Structural representation of the complex formed between transducin and the nonameric oligomer array. The optimal representative structure (defined in the Methods) is shown for model 2. (**c**) Close-up view of the interaction between specific residues of Gα (rendered in red in space filling representation) and the IL3 (cyan) and IL2 loops of protomers A and B (magenta and blue, respectively). (**d**) Side view of the complex showing $G_t\alpha$ (red), $G_t\beta$ (wheat), $G_t\gamma$ (orange), protomer A (green), protomer B (light blue), IL2 of protomer A (magenta), IL2 of protomer B (blue) and IL3 of protomer B (cyan). Other views of the model complex are shown in **Supplementary Figure 10**.

DISCUSSION

We find that agonist binding to a single protomer maximally activates a signaling unit comprising two class A GPCRs and a single G protein. Whereas activation of the second protomer inhibits the functional response, inverse agonist binding to the second protomer enhances signaling (**Fig. 6**). Our results are consistent with studies in the class C mGluR using allosteric modulators that act within the transmembrane region to show that the inactive state of a protomer

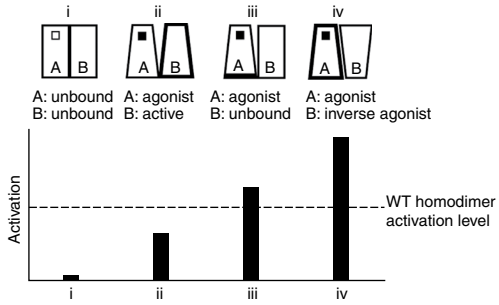

Figure 6 Cartoon of different D2R dimer activation states, with activation data for these states, from the perspective of agonist-mediated activation of protomer A. Bound agonist is represented by a black square. Activation is represented by a trapezoid with a bold base. Extent of activation is indicated by increasingly bold trapezoid boundaries. The inverse agonist bound state is represented by an inverted trapezoid. (i) Neither protomer is activated. (ii) Protomer A binds agonist and protomer B is constitutively active (or in the case of a heterodimer, is occupied by protomer B's agonist). (iii) Protomer A binds agonist, whereas protomer B cannot bind (or in a heterodimer, is not agonist-bound). Note that although protomer B is not activated by ligand, it can isomerize to the active state, which would result in configuration ii. (iv) Protomer A binds agonist, whereas protomer B is stabilized in the inactive state by inverse agonist. Experimentally determined maximal activation representing these idealized conformations: (i) no ligand, (ii) WT D2R coexpressed with D114A/CAM-G_{qi5}, (iii) WT D2R coexpressed with D114A-G_{qi5}, (iv) WT D2R coexpressed with D2/D4-G_{qi5} in the presence of the selective D4 antagonist L745,870. Activation data are normalized to that of WT D2R coexpressed with WT D2R-G_{qi5}, which is indicated by a dotted line to show the potential range of enhanced and reduced signaling achievable by modulation of the 'heterodimer' partner.

caused by inverse agonist binding results in more efficient activation of the adjacent protomer[36,37]. These findings are more difficult to reconcile with other findings in the mGluR showing that although one agonist can activate the dimeric signaling unit, two agonists are required for full activation[38], thus suggesting differences in the mechanisms of these receptors, which have very different agonist binding sites. Our findings are, however, fully consistent with the proposed function of $GABA_B$ receptors, in which only R1 binds GABA[39] with efficient signaling by the complex. A similar scenario also seems likely for rhodopsin's ability to respond to single photons, which requires robust activation by a single protomer in a dimeric unit. Indeed, in this case, the strong inverse agonist 11-*cis*-retinal (**7**) in the binding pocket of the second protomer would in fact optimize signaling, just as we observe in configuration 4 in **Figure 6**. Our findings also suggest that optimal signaling in a heteromeric GPCR would result from co-stimulation with an agonist to one protomer and an inverse agonist to the other.

Our data and models suggest that the way in which the two protomers contribute to the activated complex with the G protein is not symmetrical, and that activation requires different conformational changes in each protomer. Existing evidence for ligand-induced conformational changes in a second nonbinding protomer[13,40] is consistent with the proposal of conformational changes in both protomers. We previously demonstrated an activation-related conformational change at the TM4 dimer interface[34] that also would be consistent with movement of either one or both TM4s. Our present finding that transduction-deficient mutants in different TMs differentially affect the ability of protomer B to rescue function is consonant with the importance of conformational changes in this protomer. Notably, the apparent negative cooperativity of ligand binding observed in a number of class A GPCRs[41] may well relate to this proposed asymmetry of the signaling unit. For example, in cells expressing chemokine receptor heterodimers, a selective ligand for one protomer leads to dissociation of ligand bound to the other protomer[42], which is consistent with transmission of an altered conformation across the dimer interface and with a decreased propensity for simultaneous agonist binding to both protomers.

In summary, although a single B2AR or rhodopsin molecule can efficiently activate G proteins when reconstituted into a nanodisc, a second protomer is present *in vivo* and profoundly modulates G protein activation of the first protomer, as we have shown with our functional complementation studies. Importantly, we show that this allosteric modulation of signaling results from a direct interaction of the receptor dimer with the G protein, rather than from a downstream effect. This is likely to explain many of the surprising observations concerning the mutual modulation of heteromeric receptor oligomers by ligand binding to one protomer or the other. Moreover, we demonstrate that the constitutive activity of a protomer will modulate the activity of the dimeric signaling unit in which it participates. Thus, inverse agonists at one protomer in a heterodimer are likely to be allosteric potentiators of the signaling of its heterodimer partner, whereas agonists of one protomer will be allosteric inhibitors of the second protomer, which offers a mechanistic explanation for the often befuddling observations regarding pharmacological effects of ligands acting on heterodimers. Moreover, our model suggests that modulators might be found that are specific for heterodimers and not homodimers, but heretofore it has not been possible to screen for such compounds without the interference of homodimer-mediated signaling. Indeed, it is possible that findings of functional selectivity, that is, different agonists for a given receptor having different effects on different downstream effectors might reflect differential pharmacological effects on different heteromeric species[43]. The new methodology we present here makes it possible to identify signaling from a defined heterodimer and thus to identify modulators of heterodimer function. The modulatory mechanism we characterized and the approach that made this possible offer a new understanding of GPCR signaling in units composed of at least two GPCRs; applied to specific systems, the approach will make it possible to understand the effects of drugs that target each protomer of such a signaling unit, whether they are identical or different.

METHODS

Materials. The D2R agonist quinpirole hydrochloride and the D4R antagonist L745,870 (3-(4-[4-chlorophenyl]piperazin-1-yl)-methyl-1H-pyrrolo[2,3-b]pyridine trihydrochloride) were from Sigma-Aldrich.

DNA constructs. Expression plasmids expressing signal peptide Flag-tagged D2short WT[44] and mutant receptors were created using standard molecular biology procedures, as described in **Supplementary Methods.** Receptor constructs were fused directly through their C termini, or through an eight-amino-acid linker, to a PTX-resistant G_{qi5} (**Supplementary Fig. 2**).

Cell culture and transfection. Flp-In T-REx 293 cells (Invitrogen) were cultured and transfected, and stable lines were selected as described in **Supplementary Methods**.

Cell surface expression assay. An aliquot of the cell solution used for the aequorin assay (see below) was used to determine receptor cell surface expression as described previously[45] with anti-Flag M2 (Sigma) or anti-Myc (Mt. Sinai Medical Center hybridoma facility) as primary antibodies and R-phycoerythrin goat anti-mouse IgG (Invitrogen) as secondary antibodies using a Guava Easycyte (Guava technologies).

Aequorin assay. A functional assay based on luminescence of mitochondrial aequorin following intracellular Ca^{2+} release was performed[21,46]. Cells were seeded in a 15 cm dish and grown in antibiotic-free medium for ~48 h until mid-log phase. 1 μg ml^{-1} tetracycline was added to the medium for 3–24 h before harvest to induce the expression of the transfected D2R in pcDNA5/FRT/TO. Cells were dissociated and pelleted at 0.6 g for 3 min. After washing once with DMEM (Invitrogen) supplemented with 0.1% (w/v) bovine serum albumin, cells were resuspended in this medium at a final concentration of 5×10^6 cells ml^{-1} in the presence of 5 μM coelenterazine *h*. After 4 h rotating at room temperature (20 °C) in the dark, the cell solution was diluted tenfold, followed by 1 h incubation under the same conditions. Concentration-response curves were obtained by injecting 50 μl of cell solution into wells of a 96-well microplate containing 50 μl of a 2× concentration of the desired compound in medium. Luminescence signals from the first 15 s after injection were read by a POLARstar optima reader (BMG). Total response was defined as the signal resulting from injecting 50 μl cell solution into 50 μl assay medium containing 0.1% (v/v) triton, which raises the Ca^{2+} concentration directly by membrane permeabilization.

To normalize for different levels of surface expression levels of the Flag-D2R-G_{qi5} mutant constructs, the E_{max} at each expression level (**Supplementary Fig. 6c**) was plotted as a function of different levels of expression of Flag-tagged WT D2R-G_{qi5}, the expression of which was controlled by varying the time after tetracycline induction (**Supplementary Fig. 6a**). The level of Myc-D2R remained essentially unchanged (**Supplementary Fig. 6b**). The standard curve was fit to a one-site rectangular hyperbola using nonlinear regression in Graph Pad PRISM 4.0 (**Supplementary Fig. 6d**). The luminescence response of the various Flag-D2R-G_{qi5} constructs was normalized using this standard curve to account for the effects of different expression levels, with activation of 1 defined as that observed after 12 h of tetracycline induction of WT D2R-G_{qi5}. The Flag detection was approximately fivefold more sensitive than that of Myc; thus, the excess of Myc-tagged protomer A, which cannot signal on its own, ensures that normalization based on surface expression of the Flag-tagged G_{qi5}-fused protomer B accurately reflects the productive signaling entities, each of which must contain a protomer A and a protomer B.

Model construction. In the absence of experimentally determined structures of D2R and G_{qi5}, the templates for the oligomeric model constructs were complexes between crystallographically determined structures of rhodopsin and heterotrimeric G proteins, as described in **Supplementary Methods**. To enable the simultaneous probing of G protein interaction with different dimer arrangements, we constructed a rhodopsin oligomer composed of nine monomers. The activated form of the rhodopsin monomers used here was constructed by inclusion of all constraints reported for rhodopsin, as described previously[47]. Three dimeric interfaces were analyzed: model 1, in which the dimers have a TM4,5 interface; model 2, with a symmetric TM4 interface[34]; and model 3, in which the dimers have a TM1 interface[32].

G protein–rhodopsin docking. The docking was carried out with the HADDOCK (high ambiguity driven protein-protein docking) software[48,49]. The docking process was driven by ambiguous interaction restraints (AIRs)[48] to both monomers, as described in **Supplementary Methods**. The constraints, established from literature-derived experimental data for the binding complex, are given in **Supplementary Table 1**. Notably, the docking protocol of G_t to such models using this set of constraints was verified by the full agreement with the complex obtained for the recent structure of opsin[50] representing a putative activated form of the protein (**Supplementary Methods**). To select a second protomer for the complex, another docking run was made with restraints only to the central rhodopsin, allowing transducin to explore freely different orientations with respect to the rhodopsin oligomer. By application of the docking protocol consisting of randomization of orientations and rigid body energy minimization, 1,000 different conformations were generated. These structures were ranked according to their average interaction energies (sum of E_{elec}, E_{vdw}, E_{AIR}), screened using the 18 constraints listed in **Supplementary Table 2** (which represent the information extracted from the experimental data) and translated into Cα-Cα intermolecular constraints (**Supplementary Table 2**). Only Cα-Cα distances < 20 Å were interpreted as direct rhodopsin-G_t interactions. A cutoff of 50% fulfillment of the interaction criteria was used for accepting valid constructs. The relative probabilities of such valid G protein complexes with the various model dimers (TM4; TM4,5; TM1) were calculated from the corresponding percentages of acceptable complexes found in the resulting set of 1,000 structures retrieved from the docking procedure. The construct fulfilling the largest number of experimentally derived constraints and with the N-terminal helix of Gα parallel to the cytoplasmic face of the rhodopsin dimer was chosen as the 'optimal representative structure' for each model.

Note: Supplementary information and chemical compound information is available on the Nature Chemical Biology website.

ACKNOWLEDGMENTS

We thank C. Galés for discussion and comments on the manuscript. Plasmids encoding apo-aequorin were a gift from V. Dupriez (Euroscreen). This work was supported in part by US National Institutes of Health grants DA022413 and MH054137 (to J.A.J.) and DA012923 (to H.W.), by the Lieber Center for Schizophrenia Research and Treatment, and by a European Molecular Biology Organization long-term fellowship (to E.U.). Computational resources of the David A. Cofrin Center for Biomedical Information (Institute for Computational Biomedicine, Weill Cornell Medical College of Cornell University) are gratefully acknowledged.

AUTHOR CONTRIBUTIONS

Y.H. created all the mutant constructs and cell lines, helped to design the experiments, carried out the experimental assays and analyzed the results. I.S.M. performed the computational analysis. E.U., H.W. and J.A.J. helped to design experiments and interpret results. All the authors participated in the writing and editing of the manuscript.

Published online at http://www.nature.com/naturechemicalbiology/.
Reprints and permissions information is available online at http://npg.nature.com/reprintsandpermissions/.

1. Pin, J.P. *et al.* International Union of Basic and Clinical Pharmacology. LXVII. Recommendations for the recognition and nomenclature of G protein-coupled receptor heteromultimers. *Pharmacol. Rev.* **59**, 5–13 (2007).
2. Sartania, N., Appelbe, S., Pediani, J.D. & Milligan, G. Agonist occupancy of a single monomeric element is sufficient to cause internalization of the dimeric beta2-adrenoceptor. *Cell. Signal.* **19**, 1928–1938 (2007).
3. Parenty, G., Appelbe, S. & Milligan, G. CXCR2 chemokine receptor antagonism enhances DOP opioid receptor function via allosteric regulation of the CXCR2-DOP receptor heterodimer. *Biochem. J.* **412**, 245–256 (2008).
4. Vilardaga, J.P. *et al.* Conformational cross-talk between alpha2A-adrenergic and mu-opioid receptors controls cell signaling. *Nat. Chem. Biol.* **4**, 126–131 (2008).
5. Pin, J.P., Galvez, T. & Prezeau, L. Evolution, structure, and activation mechanism of family 3/C G-protein-coupled receptors. *Pharmacol. Ther.* **98**, 325–354 (2003).
6. Brock, C. *et al.* Activation of a dimeric metabotropic glutamate receptor by intersubunit rearrangement. *J. Biol. Chem.* **282**, 33000–33008 (2007).
7. Ji, I.H., Lee, C., Song, Y.S., Conn, P.M. & Ji, T.H. Cis- and trans-activation of hormone receptors: the LH receptor. *Mol. Endocrinol.* **16**, 1299–1308 (2002).
8. Bayburt, T.H., Leitz, A.J., Xie, G., Oprian, D.D. & Sligar, S.G. Transducin activation by nanoscale lipid bilayers containing one and two rhodopsins. *J. Biol. Chem.* **282**, 14875–14881 (2007).
9. Whorton, M.R. *et al.* A monomeric G protein-coupled receptor isolated in a high-density lipoprotein particle efficiently activates its G protein. *Proc. Natl. Acad. Sci. USA* **104**, 7682–7687 (2007).
10. George, S.R. *et al.* Oligomerization of mu- and delta-opioid receptors-generation of novel functional properties. *J. Biol. Chem.* **275**, 26128–26135 (2000).
11. Lee, S.P. *et al.* Dopamine D1 and D2 receptor co-activation generates a novel phospholipase C-mediated calcium signal. *J. Biol. Chem.* **279**, 35671–35678 (2004).
12. Guo, W., Shi, L. & Javitch, J.A. The fourth transmembrane segment forms the interface of the dopamine D2 receptor homodimer. *J. Biol. Chem.* **278**, 4385–4388 (2003).
13. Mesnier, D. & Baneres, J.L. Cooperative conformational changes in a G-protein-coupled receptor dimer, the leukotriene B4 receptor BLT1. *J. Biol. Chem.* **279**, 49664–49670 (2004).
14. Damian, M., Mary, S., Martin, A., Pin, J.P. & Baneres, J.L. G protein activation by the leukotriene B4 receptor dimer: evidence for an absence of trans-activation. *J. Biol. Chem.* **283**, 21084–21092 (2008).
15. Carrillo, J.J., Pediani, J. & Milligan, G. Dimers of class A G protein-coupled receptors function via agonist-mediated trans-activation of associated G proteins. *J. Biol. Chem.* **278**, 42578–42587 (2003).
16. Molinari, P. *et al.* Promiscuous coupling at receptor-Galpha fusion proteins. The receptor of one covalent complex interacts with the alpha -subunit of another. *J. Biol. Chem.* **278**, 15778–15788 (2003).
17. Pascal, G. & Milligan, G. Functional complementation and the analysis of opioid receptor homodimerization. *Mol. Pharmacol.* **68**, 905–915 (2005).

18. Seifert, R., Wenzel-Seifert, K. & Kobilka, B.K. GPCR-G[alpha] fusion proteins: molecular analysis of receptor-G-protein coupling. *Trends Pharmacol. Sci.* **20**, 383–389 (1999).
19. Lee, T.W., Seifert, R., Guan, X. & Kobilka, B.K. Restricting the mobility of Gs alpha: impact on receptor and effector coupling. *Biochemistry* **38**, 13801–13809 (1999).
20. Wenzel-Seifert, K., Lee, T.W., Seifert, R. & Kobilka, B.K. Restricting mobility of Gsalpha relative to the beta2-adrenoceptor enhances adenylate cyclase activity by reducing Gsalpha GTPase activity. *Biochem. J.* **334**, 519–524 (1998).
21. Rizzuto, R., Simpson, A.W.M., Brini, M. & Pozzan, T. Rapid changes of mitochondrial Ca2+ revealed by specifically targeted recombinant aequorin. *Nature* **358**, 325–327 (1992).
22. Blanpain, C. *et al.* Extracellular cysteines of CCR5 are required for chemokine binding, but dispensable for HIV-1 coreceptor activity. *J. Biol. Chem.* **274**, 18902–18908 (1999).
23. Conklin, B.R., Farfel, Z., Lustig, K.D., Julius, D. & Bourne, H.R. Substitution of three amino acids switches receptor specificity of Gq alpha to that of Gi alpha. *Nature* **363**, 274–276 (1993).
24. Miller, R.T., Masters, S.B., Sullivan, K.A., Beiderman, B. & Bourne, H.R. A mutation that prevents GTP-dependent activation of the alpha chain of Gs. *Nature* **334**, 712–715 (1988).
25. Xu, W. *et al.* Functional role of the spatial proximity of Asp114(2.50) in TMH 2 and Asn332(7.49) in TMH 7 of the mu opioid receptor. *FEBS Lett.* **447**, 318–324 (1999).
26. Ballesteros, J.A. *et al.* Activation of the beta(2)-adrenergic receptor involves disruption of an ionic lock between the cytoplasmic ends of transmembrane segments 3 and 6. *J. Biol. Chem.* **276**, 29171–29177 (2001).
27. Moro, O., Lameh, J., Hogger, P. & Sadee, W. Hydrophobic amino acid in the i2 loop plays a key role in receptor-G protein coupling. *J. Biol. Chem.* **268**, 22273–22276 (1993).
28. Strader, C.D. *et al.* Mutations that uncouple the beta-adrenergic receptor from Gs and increase agonist affinity. *J. Biol. Chem.* **262**, 16439–16443 (1987); erratum **263**, 3050 (1988).
29. Neve, K.A. *et al.* Modeling and mutational analysis of a putative sodium-binding pocket on the dopamine D-2 receptor. *Mol. Pharmacol.* **60**, 373–381 (2001).
30. Urizar, E. *et al.* An activation switch in the rhodopsin family of G protein-coupled receptors: the thyrotropin receptor. *J. Biol. Chem.* **280**, 17135–17141 (2005).
31. Simpson, M.M. *et al.* Dopamine D4/D2 receptor selectivity is determined by a divergent aromatic microdomain contained within the second, third, and seventh membrane-spanning segments. *Mol. Pharmacol.* **56**, 1116–1126 (1999).
32. Guo, W. *et al.* Dopamine D2 receptors form higher order oligomers at physiological expression levels. *EMBO J.* **27**, 2293–2304 (2008).
33. Wilson, J., Lin, H., Fu, D., Javitch, J.A. & Strange, P.G. Mechanisms of inverse agonism of antipsychotic drugs at the D2 dopamine receptor: use of a mutant D2 dopamine receptor that adopts the activated conformation. *J. Neurochem.* **77**, 493–504 (2001).
34. Guo, W., Shi, L., Filizola, M., Weinstein, H. & Javitch, J.A. From the cover: crosstalk in G protein-coupled receptors: changes at the transmembrane homodimer interface determine activation. *Proc. Natl. Acad. Sci. USA* **102**, 17495–17500 (2005).
35. Kota, P., Reeves, P.J., RajBhandary, U.L. & Khorana, H.G. Opsin is present as dimers in COS1 cells: identification of amino acids at the dimeric interface. *Proc. Natl. Acad. Sci. USA* **103**, 3054–3059 (2006).
36. Goudet, C. *et al.* Asymmetric functioning of dimeric metabotropic glutamate receptors disclosed by positive allosteric modulators. *J. Biol. Chem.* **280**, 24380–24385 (2005).
37. Hlavackova, V. *et al.* Evidence for a single heptahelical domain being turned on upon activation of a dimeric GPCR. *EMBO J.* **24**, 499–509 (2005).
38. Kniazeff, J. *et al.* Closed state of both binding domains of homodimeric mGlu receptors is required for full activity. *Nat. Struct. Mol. Biol.* **11**, 706–713 (2004).
39. Kaupmann, K. *et al.* GABAB-receptor subtypes assemble into functional heteromeric complexes. *Nature* **396**, 683–687 (1998).
40. Damian, M., Martin, A., Mesnier, D., Pin, J.P. & Baneres, J.L. Asymmetric conformational changes in a GPCR dimer controlled by G-proteins. *EMBO J.* **25**, 5693–5702 (2006).
41. Springael, J.Y., Urizar, E., Costagliola, S., Vassart, G. & Parmentier, M. Allosteric properties of G protein-coupled receptor oligomers. *Pharmacol. Ther.* **115**, 410–418 (2007).
42. Springael, J.Y. *et al.* Allosteric modulation of binding properties between units of chemokine receptor homo- and hetero-oligomers. *Mol. Pharmacol.* **69**, 1652–1661 (2006).
43. Urban, J.D. *et al.* Functional selectivity and classical concepts of quantitative pharmacology. *J. Pharmacol. Exp. Ther.* **320**, 1–13 (2007).
44. Javitch, J.A. *et al.* The fourth transmembrane segment of the dopamine D2 receptor: accessibility in the binding-site crevice and position in the transmembrane bundle. *Biochemistry* **39**, 12190–12199 (2000).
45. Costagliola, S. *et al.* Structure-function relationships of two loss-of-function mutations of the thyrotropin receptor gene. *Thyroid* **9**, 995–1000 (1999).
46. Brini, M. *et al.* Transfected aequorin in the measurement of cytosolic Ca2+ concentration ([Ca2+]c). *J. Biol. Chem.* **270**, 9896–9903 (1995).
47. Niv, M.Y., Skrabanek, L., Filizola, M. & Weinstein, H. Modeling activated states of GPCRs: the rhodopsin template. *J. Comput. Aided Mol. Des.* **20**, 437–448 (2006).
48. van Dijk, A.D. *et al.* Data-driven: HADDOCK's adventures in CAPRI. *Proteins* **60**, 232–238 (2005).
49. van Dijk, M., van Dijk, A.D., Hsu, V., Boelens, R. & Bonvin, A.M. Information-driven protein-DNA docking using HADDOCK: it is a matter of flexibility. *Nucleic Acids Res.* **34**, 3317–3325 (2006).
50. Scheerer, P. *et al.* Crystal structure of opsin in its G-protein-interacting conformation. *Nature* **455**, 497–502 (2008).

Han *et al.* 2008

Allosteric communication between protomers of dopamine Class A GPCR dimers modulates activation

Yang Han, Irina S. Moreira, Eneko Urizar,

Harel Weinstein, and Jonathan A. Javitch

Nature Chemical Biology: doi:10.1038/nchembio.199

Supplementary Figure 1

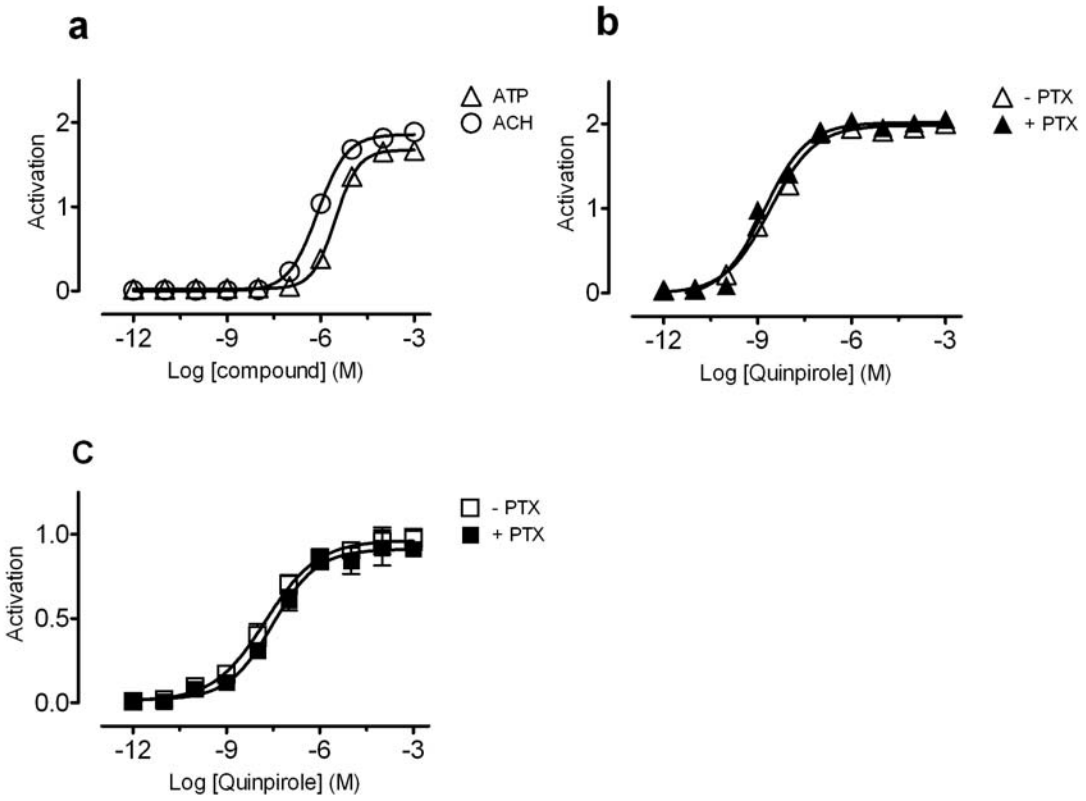

Supplementary Figure 1. *Activation of endogenous receptors and stably transfected D2R coexpressed with free Gqi5 or with D2R-Gqi5 in the presence or absence of pertussis toxin.* (**a**) Activation of Gq coupled endogenous muscarinic (ACH) and purinergic (ATP) receptors. (**b**) Activation of D2R coexpressed with free Gqi5 in the presence (▲) or absence of pertussis toxin (PTX) (Δ). (c) Activation of D2R-Gqi5 coexpressed with D2R in the presence (■) or absence of PTX (□). The mean ± SEM of 3 experiments, each conducted in triplicate, are shown.

Supplementary Figure 2

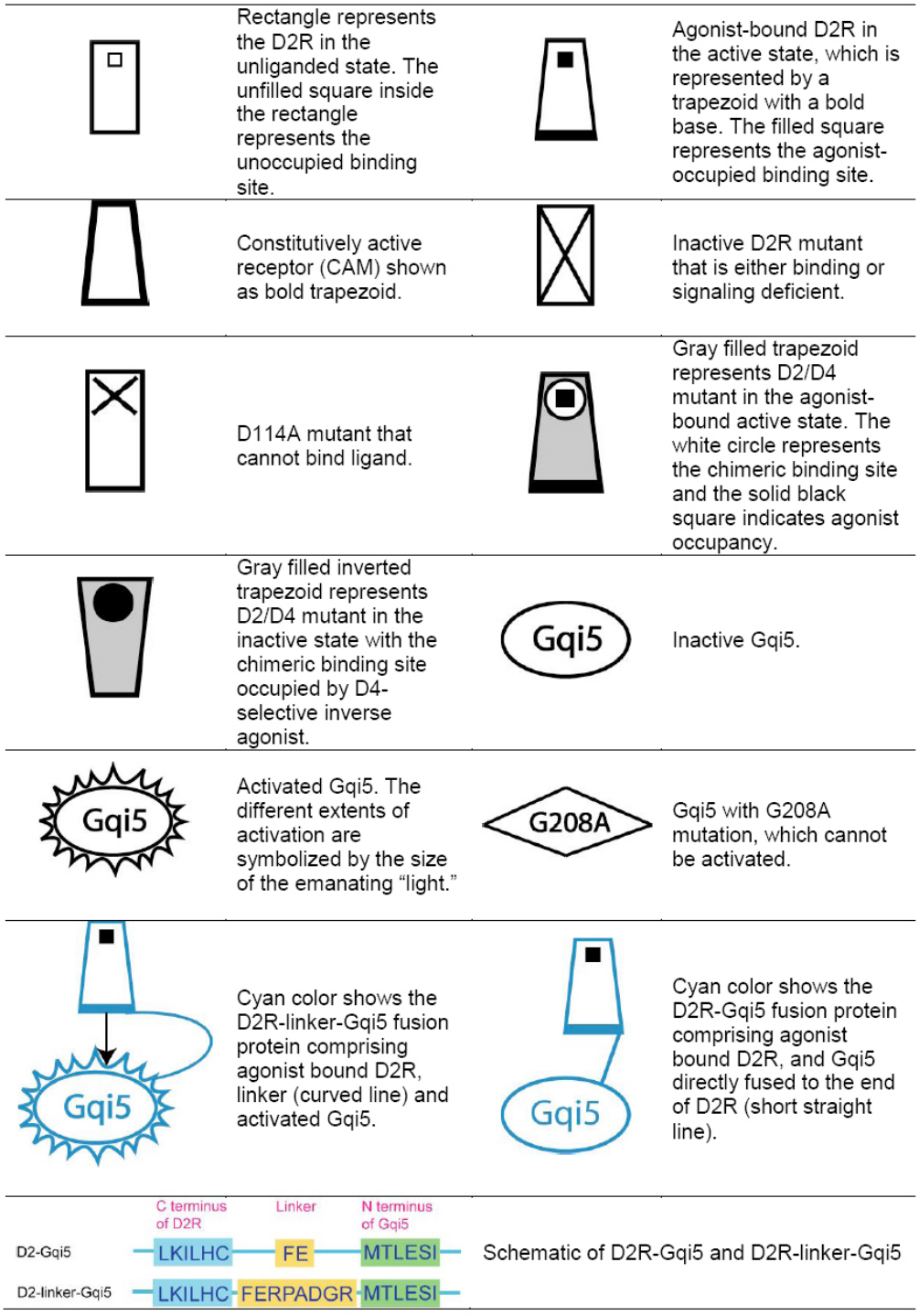

Supplementary Figure 2. *Symbols used in (**Figs. 1-4, 6** and **7**).* Schematic illustration of the sequences of the linker regions of D2R-Gqi5 and D2R-linker-Gqi5 are shown.

Supplementary Figure 3

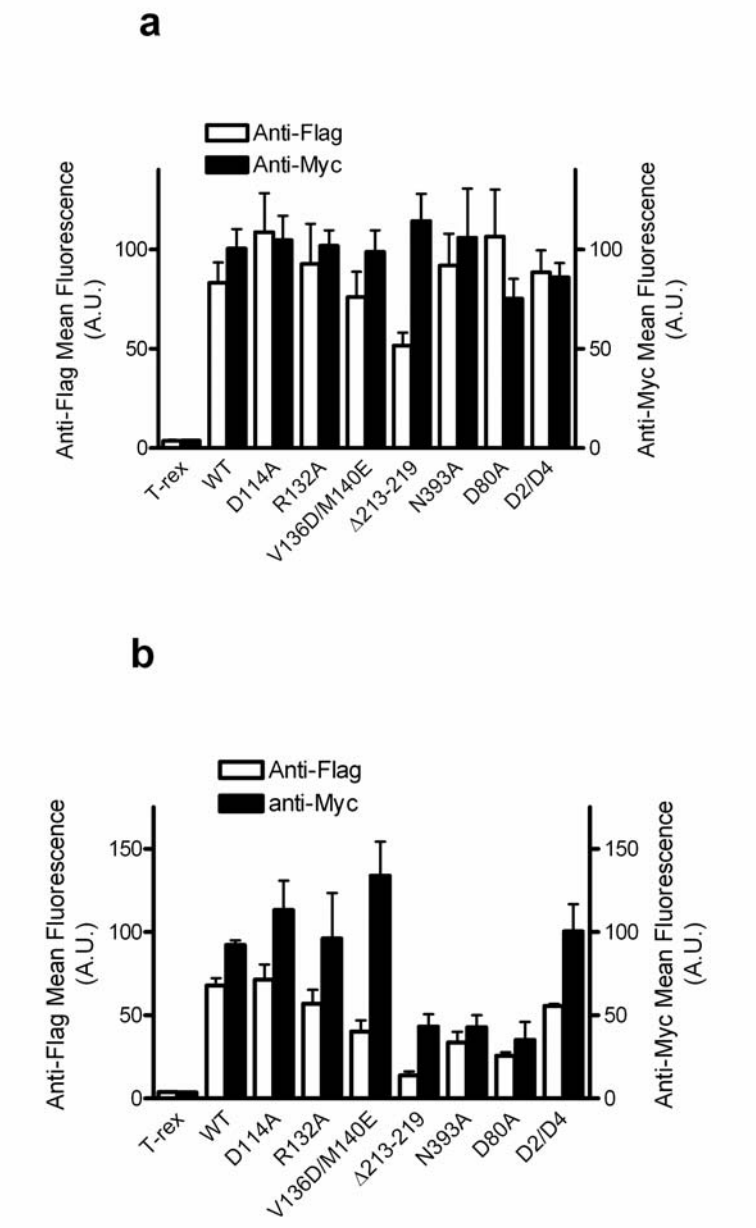

Supplementary Figure 3. *Cell surface expression of D2R WT and mutants*. (**a**) Myc-D2R mutants and Flag-D2R-Gqi5 or (**b**) Myc-D2R and Flag-D2R mutant-Gqi5 were detected by FACS (see Methods). The mean ± SEM of 3 experiments, each conducted in triplicate, are shown.

Supplementary Figure 4

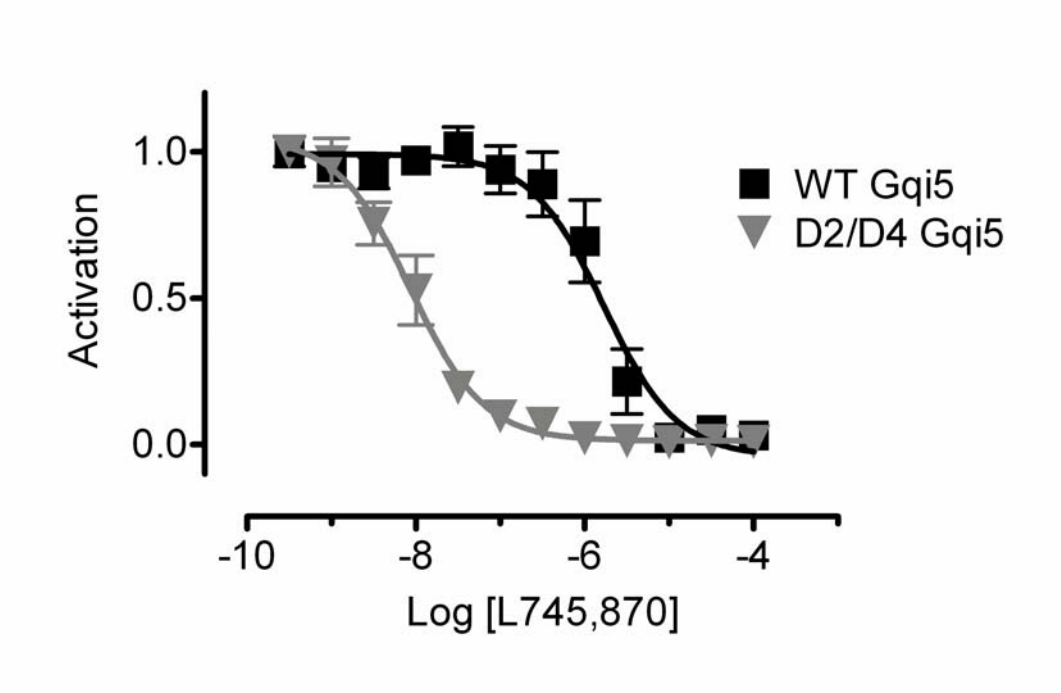

Supplementary Figure 4. *Inhibition of quinpirole-induced activation by the D4-selective antagonist L745,870 in cells in which D2R wild type or the D2/D4 mutant were coexpressed with free Gqi5*. Due to the much lower EC_{50} of the D2/D4 mutant for quinpirole, 10nM and 100 μM quinpirole were used with WT and the D2/D4 mutant, respectively, in order to achieve similar extents of activation. The mean ± SEM of 3 experiments, each conducted in triplicate, are shown.

Supplementary Figure 5

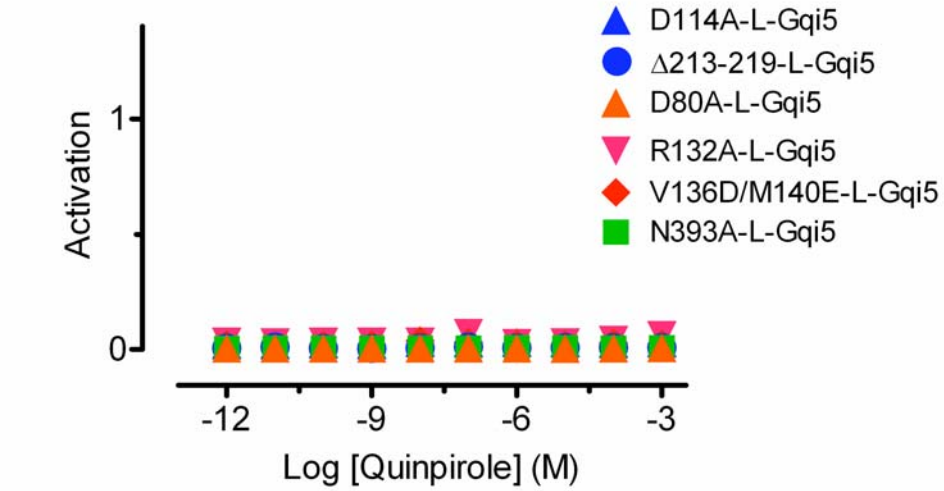

Supplementary Figure 5. *Activation of D2R mutant-linker-Gqi5.* All mutants including D114$^{3.32}$A-linker-Gqi5 (▲), deletion 213-219-linker-Gqi5 (●), D80$^{2.50}$A-linker-Gqi5 (▲), R132$^{3.50}$A-linker-Gqi5 (▼), V136$^{3.54}$D/M140$^{3.58}$E-linker-Gqi5 (♦), or N393$^{7.49}$A-linker-Gqi5 (■) failed to signal. The mean ± SEM of 3 experiments, each conducted in triplicate, are shown.

Supplementary Figure 6

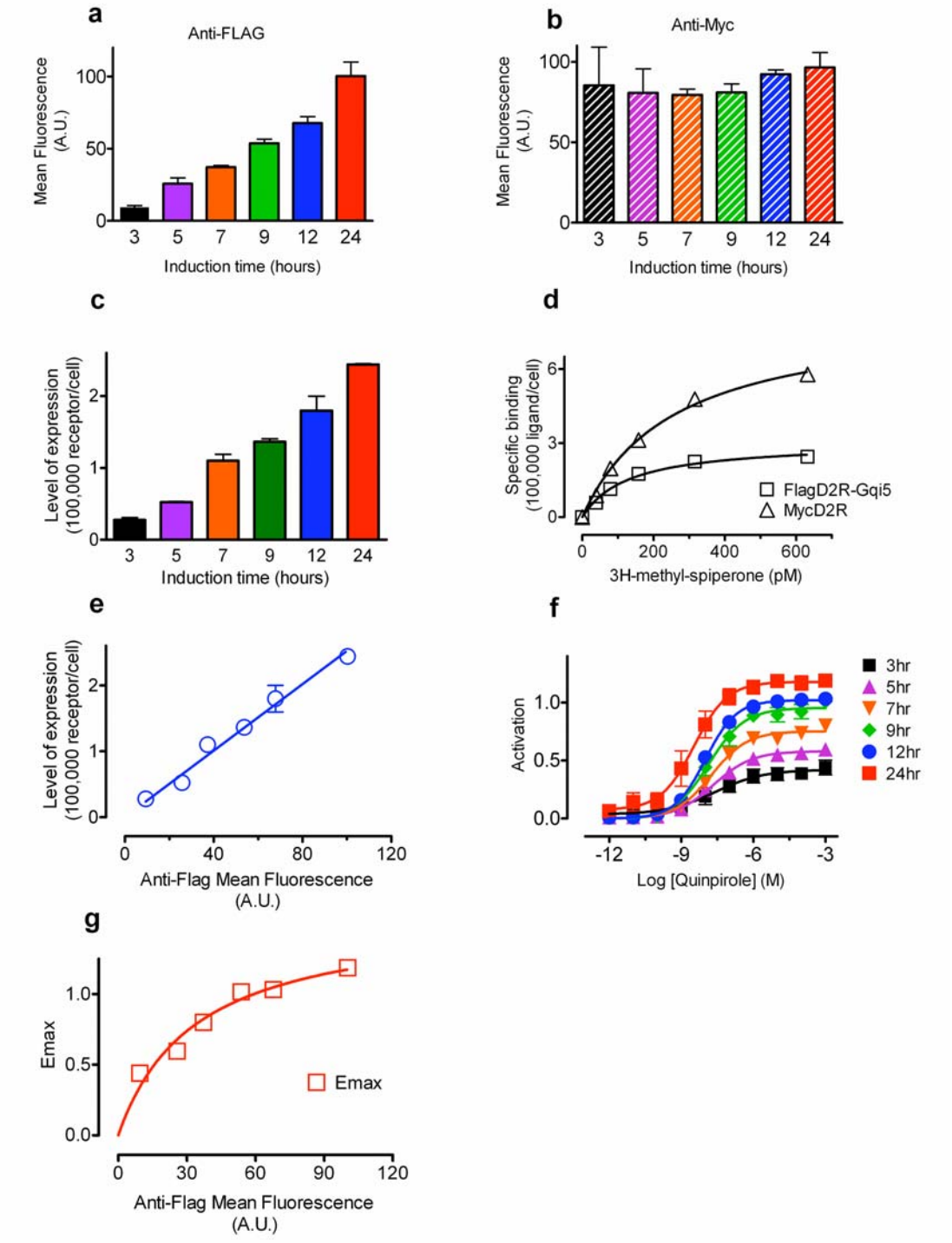

Supplementary Figure 6. *Relationship of surface expression and activation.* Surface expression was determined by FACS (see Methods) for (**a**) Flag-D2R-Gqi5, stably transfected in pcDNA5/FRT/TO (Invitrogen) and with its expression controlled by varying the length of time after tetracycline induction from 3 hours to 24 hours and for (**b**) Myc-D2R stably transfected in pIRESpuro3 vector (BD life science) and expressed constitutively. (**c**) Cells stably transfected with Flag-D2R-Gqi5 in pcDNA5/FRT/TO were induced by tetracycline for 3 to 24 hours. Specific binding of [^{3}H]*N*-methylspiperone (**8**) (0.6 nM) was determined at each time point by subtracting nonspecific binding in the presence of 1 μM sulpiride (**9**) from the total binding. This concentration was chosen based on (**d**) to estimate the Bmax of binding, which was converted to sites/cell based on the specific activity of the ligand, the efficiency of the scintillation counter, and cell counting. (**d**) Flag-D2R-Gqi5 (in pcDNA5/FRT/TO) or Myc-D2R (in pIRESpuro3) were separately stably transfected in Flp-In T-Rex cells. After 24 hours of induction with tetracycline, cells expressing Flag-D2R-Gqi5 were harvested for saturation binding assay. Cells continuously expressing Myc-D2R were harvested for saturation binding assay when suitable confluence was achieved. Saturation binding assays were performed as described in Supplementary Methods. (**e**) Linear correlation between surface receptor expression determined by FACS (**a**) and by ligand binding (**c**). (**f**) The maximal responses of D2R coexpressed with D2-Gqi5 after different periods of tetracycline induction. (**g**) These maximal responses were plotted against the surface expression level of D2-Gqi5. The standard curve was fit by nonlinear regression with the equation Y=Bmax*X/(Kd+X) using Graph Pad prism 4.0, and was used to normalize activation according to surface expression as described in Methods. The mean ±SEM of 3 experiments, each conducted in triplicate, are shown.

Supplementary Figure 7

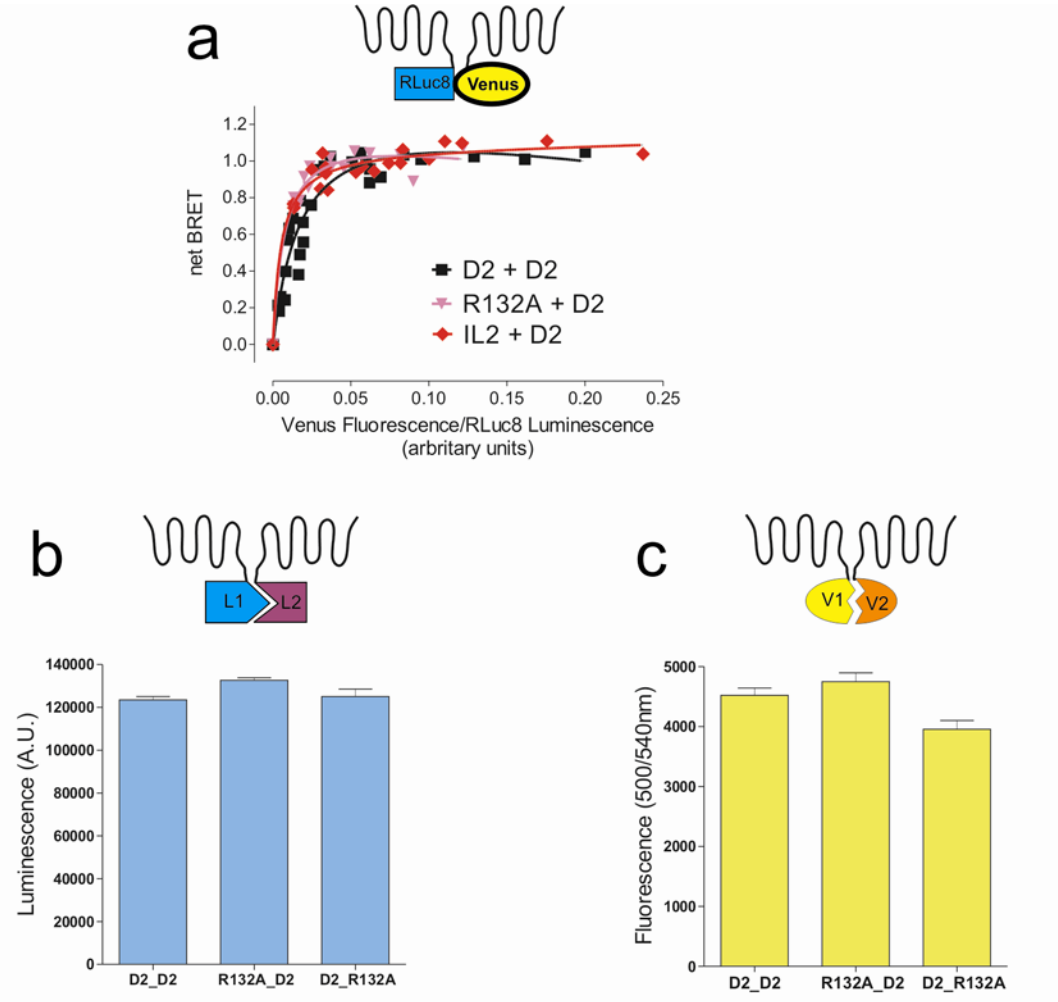

Supplementary Figure 7. *IL2 mutants interact with the WT receptor.*
(**a**) Titration BRET experiments: Increasing amounts of D2-Venus were coexpressed with constant amounts of either WT or mutant D2-RLuc8 in HEK 293T cells. 48h post-transfection BRET was performed[1]. BRET signals were plotted against the relative expression levels of each tagged receptor. Results were analyzed by non-linear regression assuming a model with one site binding (Graph Pad Prism 4.0) on a pooled data set from 2 independent experiments. HEK 293T cells transiently coexpressing WT or mutant D2R split RLuc8 (**b**) or Venus (**c**) were harvested 48 h post-transfection, washed with PBS, centrifuged and resuspended in PBS. Fluorescence was recorded for 1s using 500nm excitation and 540nm emission filters (Polarstar, BMG). Unfiltered luminescence was recorded for 1s (Gain 3900). Background was determined with cells expressing only one of the receptor probes and the signal to noise ratio was plotted for cells showing comparable cell surface level of expression for each protomer determined by FACS analysis. The graph is representative of 3 independent experiments performed with triplicate samples.

Supplementary Figure 8

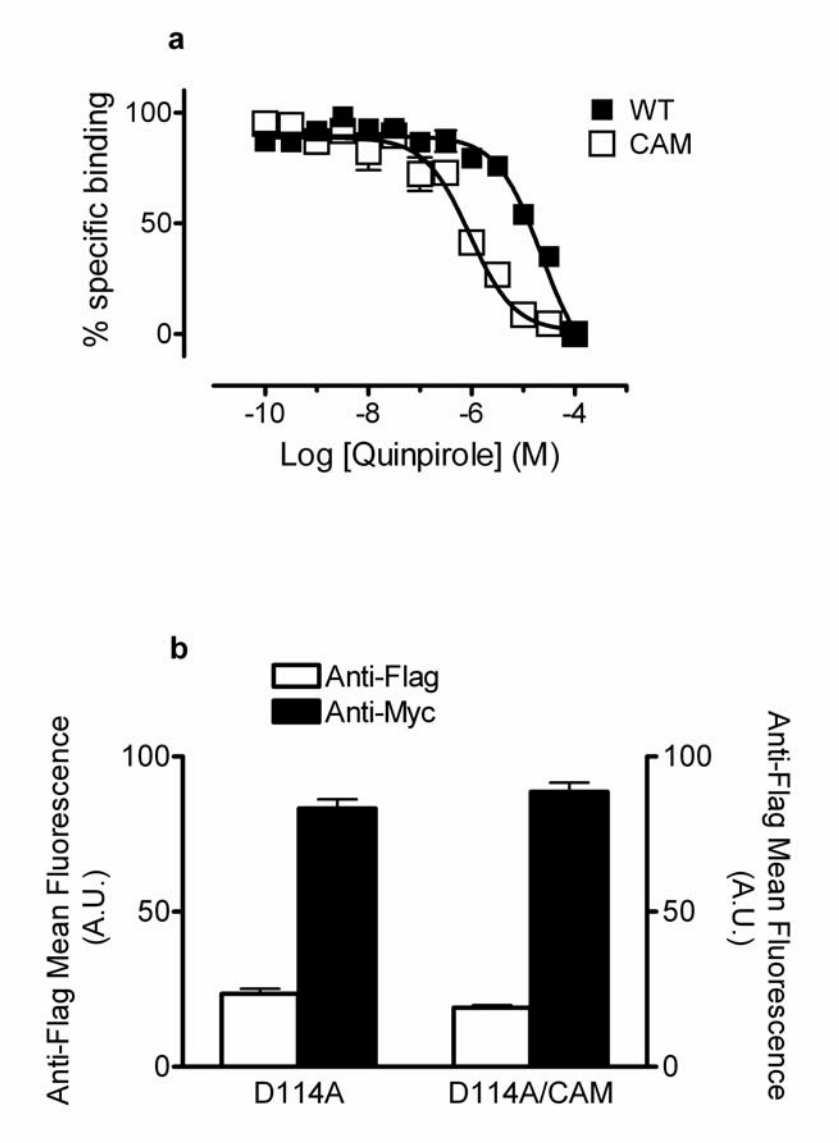

Supplementary Figure 8. *D2R E339A/T343R is constitutively active.* (**a**) The inhibitory potency of quinpirole in competition with [^{3}H]*N*-methylspiperone binding is greatly increased in D2R E339A/T343R compared to WT, consistent with its constitutive activation. Dissociation constants (K_i) of quinpirole binding were 22.45±4.0 μM and 0.913±0.19 μM for WT and the E339A/T343R mutant, respectively. (**b**) Comparable cell surface expression of coexpressed Flag-D114A-Gqi5 or Flag-D114A/CAM-Gqi5 with Myc-D2R was shown by FACS (see Methods). The mean ±SEM of 3 experiments, each conducted in triplicate, are shown.

Supplementary Figure 9

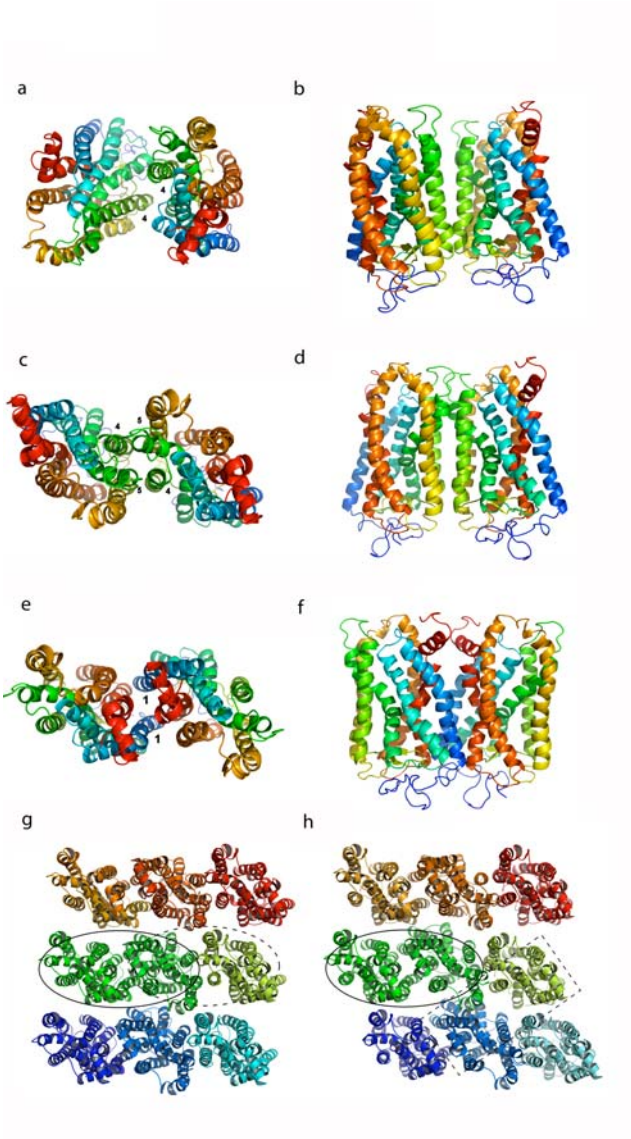

Supplementary Figure 9. *Structural representation of the dimer interfaces.* (**a** and **b**) TM4 dimer interface; (**c** and **d**) TM4,5 interface; (e and f) TM1 dimer interface. The paired panels (**a**) and (**b**), (**c**) and (**d**), (**e**) and (**f**), present top and lateral views of the dimers, respectively. Panels g and h show the nonameric oligomer array, with the various interfaces termed TM1 dimer, TM4,5 dimer, and TM4 dimer indicated by a solid ellipse, a dashed ellipse, and a dashed box, respectively.

Supplementary Figure 10

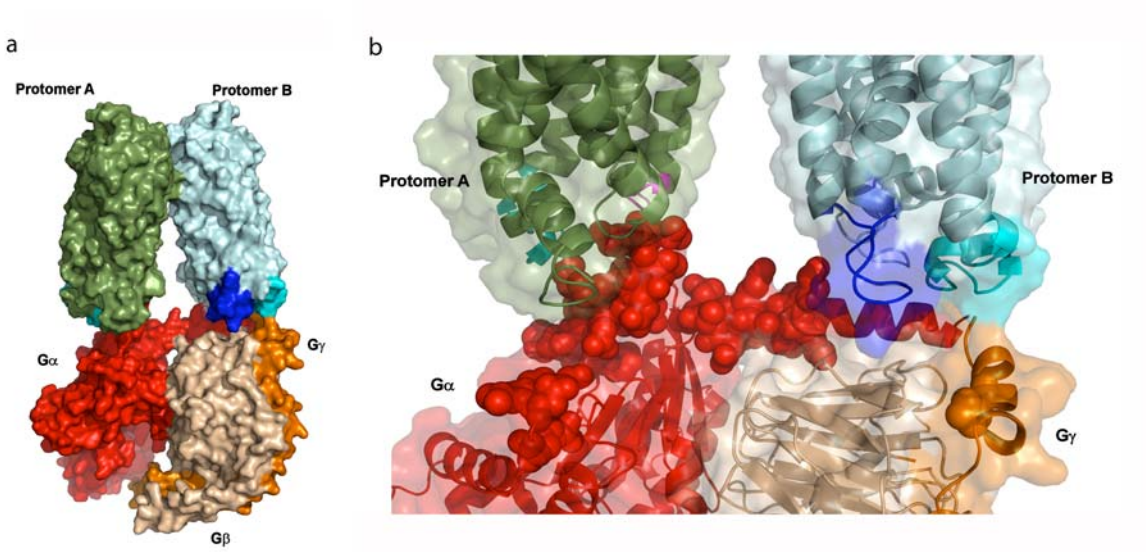

Supplementary Figure 10. *Model of the functional complex between the rhodopsin dimer and heterotrimeric Gt for the optimal representative of Model 2* (different views of the same construct as Figure 5 in the main text). (**a**) Side view of the complex showing Gtα (red), Gtβ (wheat), Gtγ (orange), protomer A (green), protomer B (light blue), IL2 of protomer A (magenta), IL2 of protomer B (blue), and IL3 of protmer B (cyan). (**b**) Closeup view of the interaction between specific residues of Gα (red, CPK representation) and the IL3 (cyan) and IL2 loops of protomers A and B (magenta and blue, respectively).

Supplementary Table 1

Protein	Residues and Positions	Reference
Gtα	V214, R309, D311, V312, K313, F330, F332, D337, I338, I340, K341, N343, L344, G348, L349, F350	[2,3]
Gtα	C347	[4]
Gtγ	N62A, P63A, F64A	[5]
Gtα	L19–R28	[6,7]
RHO	Y136 (3.51), V137 (3.52), V138 (3.53), V139(3.54)	[8]
RHO	C140 (3.55), K141 (3.66), R147 (3.72), F148 (3.73)	[9]
RHO	T229 (5.64), V230 (5.65), A233 (5.68), A234 (5.69), S240 (6.23), T242 (6.25), T243 (6.26), Q244 (6.27)	[9-11]
RHO	E247 (6.30), K248 (6.31), E249 (6.32)	[8]
RHO	N310 (7.57), K311 (7.58), Q312 (7.59)	[8,12,13]

Supplementary Table 1. Residues at the rhodopsin-transducin interface, derived from the literature-derived experimental data for the binding complex.

Supplementary Table 2

Set	RHO	Transducin	Model 1	Model 2
1	R135A	F350α	***25*** <26>	***18*** <25>
	V137A	F350 α	***20*** <29>	***16*** <29>
	S144A	D337 α	***18*** <33>	***11*** <30>
	N145A	F350 α	***11*** <29>	***7*** <21>
	T229A	F350 α	***19*** <29>	***15*** <21>
	S240A	E342 α	***13*** <34>	***11*** <20>
		N343 α	***9*** <33>	***12*** <18>
		L344 α	***6*** <33>	***8*** <19>
		N345 α	***11*** <33>	***8*** <18>
		K313 α	***22*** <38>	***18*** <26>
	E247A	F350 α	***13*** <39>	***13*** <21>
	E249A	L344 α	***21*** <46>	***23*** <18>
2	K141A	R28 α	***12*** <26>	***19*** <20>
	S240A	K28 α	***12*** <32>	***18*** <17>
	K248A	L19 α	***25*** <41>	***28*** <24>
3	R147	A23 α	***17*** <23>	***21*** <16>
	S240B	L19 α	***14*** <19>	***18*** <17>
		A23 α	***14*** <16>	***21*** <12>
	C316B	P63 γ	***38*** <41>	***36*** <36>

Supplementary Table 2. Literature-derived constraints used in the construction of the models for rhodopsin-transducin complexes. The distance (in Å) between the Cα of specific residues of rhodopsin and transducin for the two studied models is shown in bold italics. Numbers in brackets are the average distances from the docking solutions from which the optimal representatives were chosen as Model 1 (TM4, 5 dimer) and Model 2 (TM4 dimer) as described in Methods. Set 1 refers to the interactions of the C terminus of Ga with protomer A, set 2 refers to the interactions between the N terminus of Ga and protomer A, and set 3 refers to the interactions between the N terminus of Ga and protomer B.

Supplementary Methods

Numbering of residues. Residues are numbered both according to their positions in the human D2short receptor (D2R) sequence and also relative to the most conserved residue in the TM in which they are located[14]. The most conserved residue in each TM is assigned the position index '50', for example, in TM3, Arg132$^{3.50}$, and therefore Asp131$^{3.49}$ and Ty133$^{3.51}$.

DNA constructs. The stop codons in the Signal Peptide Flag-tagged D2short WT[15] and mutant receptors were removed by PCR, and the sequence TTCGAA was inserted in place of the D2R stop codon to create a BstBI site. Gαqi5 (referred to as Gqi5) was constructed by replacing the last 5 amino acids of Gαq by those of $G\alpha i_1$, except that the Cys four residues from the C-terminus was mutated to Ile, rendering Gαi pertussis-toxin resistant[16]. The sequence TTCGAA was also inserted immediately priority to the start codon of Gqi5. D2R-Gqi5 (schematic illustration shown in **Supplementary Fig. 2**) was made by subcloning the two fragments using the BstBI site. D2R-linker-Gqi5 (schematic illustration shown in **Supplementary Fig. 2**) was made by inserting the additional sequence TTCGAAAGACCTGCAGACGGTAGA, which encodes FERPADGR as a linker, between the D2R last amino acid and the start codon of Gqi5. For D2R-linker-Gqi5G208A, G208A was mutated by PCR, which resulted in nonfunctional Gα[17]. Flag-tagged D2R, D2R-Gqi5 and D2R-linker-Gqi5 were subcloned into pcDNA5/FRT/TO (Invitrogen). cDNA encoding Myc-tagged D2R and Gqi5 were

subcloned into the pIRESpuro3 vector (Clontech). Plasmids encoding apoaequorin were a gift from Vincent J. Dupriez (Euroscreen, Belgium), and were subcloned into the pCIN4 plasmid[15] to create pCIN4AEQ.

Cell culture and transfection. Flp-In T-REx 293 cells (Invitrogen) were maintained in DMEM medium (GIBCO) supplemented with 10% (v/v) FBS (Gemini) and 2 mM L-glutamine (Invitrogen). Cells were transfected with Lipofectamine 2000 (Invitrogen) according to the manufacturer's protocol. pCIN4AEQ was transfected into Flp-In T-REx 293 cells, followed by G418 (Mediatech) selection. Single colonies were isolated, and a clone was identified in which acetylcholine-induced activation of endogenous muscarinic M1 receptors (which couple to endogenous Gq) resulted in robust luminescence in the presence of coelenterazine *h* (Byosinth, Switzerland) (see below). This parental aequorin cell line was transfected with unfused Myc-tagged D2R in pIRESpuro3 followed by puromycin (Sigma-Aldrich) selection. After selection, cells were transfected with Flag-tagged D2R-Gqi5 fusion in pcDNA5/FRT/TO, followed by hygromycin b (Mediatech) selection. Stable coexpression of unfused D2R with unfused Gqi5 was achieved by the same strategy. When noted, cells were treated with 100 ng/ml pertussis toxin (Sigma-Aldrich) for 16-24 hours prior to harvest.

Saturation and competition binding. Cells expressing Flag-D2R-Gqi5 were harvested after induction by tetracycline for varying time from 3 to 24 hours. Cells continuously expressing Myc-D2R were harvested when confluence was suitable. Binding studies were carried out with [^{3}H]*N*-methylspiperone (PerkinElmer Life

Sciences) using 1 μM sulpiride (Sigma-Aldrich) to define nonspecific binding, as described previously[18]. Cells coexpressing D2R or D2R E339A/T343R with free Gqi5 were induced for 20 hours prior competition binding assay. Intact cells were harvested for binding and [^{3}H]*N*-methylspiperone binding was performed as described previously[18].

Molecular Constructs. The Gtα subunit of bovine transducin was built with homology modeling using the MODELLER software[19] and the crystal structure of the complex of a Gtα/Giα chimera and the Gtβγ subunits (PDBID: 1GOT)[20] as templates. As the very important C-terminal residues of Gtα (residues 340-350) were missing from the resulting complex, we grafted to this structure the "activated peptide" of Gt (PDBID: 1LVZ)[21]. This required a patching of the Ile340-Glu342 segment and restoration of Cys347. The 1GOT structure of the heterotrimeric Gtαβγ was used to model the Gβγ subunit. As the last residues of Gtγ were missing, we used the same approach as described above to complete the structure: the Gtγ (60-71) farnesyl dodecapeptide (PDBID: 1MF6)[5] in complex with an activated rhodopsin was grafted to the Gt modeled by overlapping Asp60-Asn62. Energy minimization of the Gαβγ was then performed using the AMBER force field[22].

Constrained docking procedure. Application of the experimentally-derived constraints took advantage of the distinction made by the HADDOCK algorithm between "active" and "passive" residues. The "active" residues are those considered to be involved in the interaction between the two molecules (**Supplementary Table 2**) and to be solvent accessible (either main chain or side

chain relative accessibility should be typically >40-50%, which is calculated with the software NACCESS[23]). The "passive" residues are all solvent accessible surface neighbors of active residues. An ambiguous interaction restraint (AIR), the maximum distance between any atom of an active residue of one molecule to any atom of an active or passive residue of the second molecule has a maximum value of 3 Á, as the effective distance d_{eff} will always be shorter than the shortest distance entering the sum: $d_{eff}=[Sum(1/r^6)]^{1/6}$.

The crystal structure of opsin (Ops*) in complex with the GαCT (340-350) segment published recently[24] provided an opportunity for validation of our docking procedure for a cognate monomer in a proposed activated form. Using the computational protocol described in the main text, we docked the component structures and scored them according to our interaction criteria described in the Methods. The structures chosen based on these criteria present Root Mean Square Deviations (RMSD) values lower than 2.5 Å in comparison to the crystallographic complex (PDBID: 3DQB)[24], positioning the GαCT ligand in exactly the same binding crevice as observed in the crystal structure. These results confirm the applicability of the procedure and the scoring criteria used to dock the Gt protein.

Reference List

1. Guo, W. *et al.* Dopamine D2 receptors form higher order oligomers at physiological expression levels. *EMBO J.* (2008).

2. Onrust, R. *et al.* Receptor and beta gamma binding sites in the alpha subunit of the retinal G protein transducin. *Science.* **275**, 381-384 (1997).

3. Osawa, S. & Weiss, E. R. The effect of carboxyl-terminal mutagenesis of Gt alpha on rhodopsin and guanine nucleotide binding. *J. Biol. Chem.* **270**, 31052-31058 (1995).

4. Arimoto, R., Kisselev O.G., Makara G.M. & Marshall G.R. Rhodopsin-transducin interface; studies with conformationally constrained peptides. *Biophys. J.* **81**, 3285-3293 (2001).

5. Kisselev, O. G. & Downs, M. A. Rhodopsin-interacting surface of the transducin gamma subunit. *Biochemistry* **45**, 9386-9392 (2006).

6. Cai, K., Itoh, Y. & Khorana, H. G. Mapping of contact sites in complex formation between transducin and light-activated rhodopsin by covalent crosslinking: use of a photoactivatable reagent. *Proc. Natl. Acad. Sci. U S A.* **98**, 4877-4882 (2001).

7. Itoh, Y., Cai, K. & Khorana, H. G. Mapping of contact sites in complex formation between light-activated rhodopsin and transducin by covalent crosslinking: Use of a chemically preactivated reagent. *PNAS* **98**, 4883-4887 (2001).

8. Acharya, S., Saad, Y. & Karnik, S. S. Transducin-alpha C-terminal peptide binding site consists of C-D and E-F loops of rhodopsin. *J. Biol. Chem.* **272**, 6519-6524 (1997).

9. Natochin, M., Gasimov, K. G., Moussaif, M. & Artemyev, N. O. Rhodopsin determinants for transducin activation; a gain-of-function approach. *J. Biol. Chem.* **278**, 37574-37581 (2003).

10. Janz, J. M. & Farrens, D. L. Rhodopsin activation exposes a key hydrophobic binding site for the transducin alpha-subunit C terminus. *J. Biol. Chem.* **279**, 29767-29773 (2004).

11. Yang, K., Farrens, D. L., Hubbell, W. L. & Khorana, H. G. Structure and function in . Single cysteine substitution mutants in the cytoplasmic interhelical E-F loop region show position-specific effects in transducin activation. *Biochemistry* **35**, 12464-12469 (1996).

12. Ernst, O. P. *et al.* Mutation of the fourth cytoplasmic loop of rhodopsin affects binding of transducin and peptides derived from the carboxyl-terminal sequences of transducin alpha and gamma subunits. *J. Biol. Chem.* **275**, 1937-1943 (2000).

13. Marin, E. P. *et al.* The terminus of the fourth cytoplasmic loop of rhodopsin modulates rhodopsin-transducin interaction. *J. Biol. Chem.* **275**, 1930-1936 (2000).

14. Ballesteros, J. A. & Weinstein, H. [19] Integrated methods for the construction of three-dimensional models and computational probing of structure-function relations in G protein-coupled receptors. *Methods Neurosci.* **25**, 366-428 (1995).

15. Javitch, J. A. *et al.* The fourth transmembrane segment of the dopamine D2 receptor: Accessibility in the binding-site crevice and position in the transmembrane bundle. *Biochemistry* **39**, 12190-12199 (2000).

16. Wise, A. *et al.* A Cysteine-3 to Serine Mutation of the G-Protein Gi1 alpha Abrogates Functional Activation by the alpha 2A-Adrenoceptor but Not Interactions with the beta gamma Complex. *Biochemistry* **36**, 10620-10629 (1997).

17. Miller, R. T., Masters, S. B., Sullivan, K. A., Beiderman, B. & Bourne.H.R. A mutation that prevents GTP-dependent activation of the alpha chain of Gs. *Nature* **334**, 712-715 (1988).

18. Javitch, J. A., Fu, D. & Chen, J. Residues in the fifth membrane-spanning segment of the dopamine D2 receptor exposed in the binding-site crevice. *Biochemistry* **34**, 16433-16439 (1995).

19. Martin-Renom, M. A. *et al.* Comparative protein structure modeling of genes and genomes. *Annu Rev Biophys Biomol Struct* **29**, 291-325 (2000).

20. Lambright, D. G. *et al.* The 2.0 A crystal structure of a heterotrimeric G protein. *Nature* **379**, 311-319 (1996).

21. Koenig, B. W. *et al.* Structure and orientation of a G protein fragment in the receptor bound state from residual dipolar couplings. *J. Mol. Biol.* **322**, 441-446 (2002).

22. Case, D. A. *et al.* The Amber biomolecular simulation programs. *J Comput. Chem.* **26**, 1668-1688 (2005).

23. Hubbard, S. J. & Thornton, J. M. 'NACCESS', computer program. *Depertment of BIochemistry Molecular Biology, University College London* (1993).

24. Scheerer, P. *et al.* Crystal structure of opsin in its G-protein-interacting conformation. *Nature* **455**, 497-502 (2008).